Tôhoku Geophys. Journ. (Sci. Rep. Tôhoku Univ., Ser. 5), Vol. 36, No. 3, pp. 311-356, 2002

Seismic Reflection Survey in Nagamachi-Rifu Fault, Sendai, Northeastern Japan

RESEACH GROUP FOR DEEP STRUCTURE OF NAGAMACHI-RIFU FAULT*

Research Center for Prediction of Earthquakes and Volcanic Eruptions,
Graduate School of Science, Tohoku University, Aoba-ku, Sendai, 980-8578

(Received January 7, 2002 ; revised January 29, 2002 ; accepted January 31, 2002)

Abstract : On September 15, 1998, an earthquake with $M5.0$ occurred at 12 km depth beneath Sendai City, northeastern Japan, and caused slight damages in the city. The epicenter of this earthquake was located about 10 km to the northwest of the Nagamachi-Rifu fault, an active fault running through the middle of the urban area of Sendai City in the NE-SW direction. By using reflected S-waves observed in seismograms of the aftershocks, distinct S-wave reflectors (bright spots) were located beneath the focal area of this earthquake. A seismic reflection/refraction experiment was conducted around the Nagamachi-Rifu fault in June, 2001. We observed 15 chemical explosions and VIBROSEIS signals by a crisscross seismic array composed by 368 off-line data recorders deployed on the hanging wall side of the fault. Predominant reflection events were observed at about 5 sec in two-way travel-time on some shot gather record sections. They correspond to the reflection from the deep structure of the Nagamachi-Rifu fault. Moreover, reflection events were also observed at about 6-7 sec in two-way travel-time, which were probably caused by the reflections from the S-wave reflectors (bright spots).

1. Introduction

Seismic reflection/refraction experiments around the Nagamachi-Rifu fault, northeastern Japan, were conducted as a part of a comprehensive joint research project "Modeling of Deep Slip Processes in Seismogenic Inland Faults". The purpose of the experiments is to reveal deep structures of the fault, such as the geometry of the fault

* Members of Research Group for Deep Structure of Nagamachi-Rifu Fault
Authors of the report : Norihito Umino, Akira Hasegawa (Tohoku Univ.)
Participants in field observation : Takeo Moriya, Ken Otsuka, Taka'aki Taira (Hokkaido Univ.), Tomoki Tsutsui, Katsuyuki Kobayashi (Akita Univ.), Akiko Hasemi, Tomotsugu Demachi, Kaoru Takizawa, Mari Ishizawa, Takeo Shibuya, Yoshinori Yajima (Yamagata Univ.), Akira Hasegawa, Norihito Umino, Toru Matsuzawa, Tomomi Okada, Ayako Nakamura, Toshiya Sato, Shuichiro Hori, Toshio Kono, Koichi Nida, Takashi Nakayama, Youichi Asano, Junichi Nakajima, Namiko Sato, Naoki Uchida, Yoko Suwa, Kazuo Yoshimoto, Hisashi Nakahara, Hideki Ueda, Tatsuhiko Saito, Sachiko Tanaka, Takuto Maeda, Tsutomu Takahashi (Tohoku Univ.), Masaki Kanao (National Institute of Polar Research), Mikiya Yamashita (The Graduate Univ. for Advanced Studies), Takaya Iwasaki, Takashi Iidaka, Yoichiro Ichinose, Mamoru Saka, Kaname Sakai, Izumi Ogino, Masato Serizawa, Keiji Adachi (Univ. of Tokyo), Toshikazu Tanada (Hot Springs Research Institute of Kanagawa Prefecture), Fumihito Yamazaki, Mamoru Yamada, Koji Aizawa (Nagoya Univ.), Shigeru Toda (Aichi Univ. of Education), Kiyoshi Ito, Kazuo Matsumura, Hiroo Wada, Setsuro Nakao, Koji Yoshii, Tomotake Ueno (Kyoto Univ.), Dapeng Zhao, Ryohei Sanda, Toshiyuki Nishino, Takeshi Ono, Om P. Mishra, Inmaculada Serrano, Mohamed K. Salah (Ehime Univ.), Hiroki Miyamachi, Shuichiro Hirano, Naoki Hayashimoto (Kagoshima Univ.)

in the seismogenic upper crust, its deeper extension in the lower crust, and seismic-wave reflectors (bright spots) around it (Hasegawa *et al.*, 2001a). Such information is necessary for modeling the deep slip processes in seismogenic inland fault system. As is the case for the vast majority of active faults, however, very little information is available regarding the deep structure of the Nagamachi-Rifu fault. The Nagamachi-Rifu fault is an active fault zone of reverse fault type, which runs the middle of the urban area of Sendai City in the NE-SW direction. The fault is about 15 km long, and its slip rate is estimated to be 0.6-1.0 m/ka (Active Fault Research Group, 1991). It is inferred that the most recent activity of this fault was 3000-2500 years ago (Otsuki, 1999).

An M5.0 earthquake of reverse-fault type occurred beneath the Ayashi area of Sendai City on September 15, 1998, and it caused slight damage to houses and roads in the city. The hypocenter of the earthquake was located at a depth of about 12 km, about 10 km to the northwest of the surface trace of the Nagamachi-Rifu fault (see Fig. 1). Focal mechanism of the M5.0 event determined by P-wave polarity data is a reverse fault type with a nearly horizontal P-axis in the NW-SE direction. Umino *et al.* (1999) relocated hypocenters of the main shock and aftershocks by the homogeneous station method (Ansel and Smith, 1975). They are shown by a star and small open circles in Fig. 1. Most of aftershocks were distributed on a 3 km×3 km plane dipping about 30 degree to the northwest. The hypocenter of the main shock was located at the lower edge of the focal area. From the relationship between the distribution of hypocenters, the focal mechanism of the main shock and the location of the surface trace of the Nagamachi-Rifu fault, the M5.0 earthquake is interpreted to have ruptured the deepest portion of the fault (Umino *et al.*, 1999).

Recent activity of microearthquakes around the Nagamachi-Rifu fault has been studied by temporary seismic observations (Yoshimoto *et al.*, 2000) and by Tohoku University seismic network data (Hasegawa *et al.*, 2001b). The results show that microearthquake activity for the last 20 years or so concentrates in the hanging wall side of the Nagamachi-Rifu fault.

A number of prominent reflected S-waves (SxS phases) were observed in seismograms of foreshocks and aftershocks of the 1998 M5.0 earthquake at many stations surrounding its focal area (Hori *et al.*, 1999). They have similar features to those of the SxS phases widely detected in the midcrust of northeastern Japan (Hasegawa *et al.*, 1991, 2000). Based on the analysis of SxS phases, several S-wave reflectors (bright spots) are located around the deep extension of the Nagamachi-Rifu fault and in the lower crust directly below it. The locations of these reflectors are shown by short straight lines in Fig. 1(b). Moreover, another predominant reflector is located below the fault plane of the M 5.0 event at depths of 15-22 km by using the arrival time differences at several nearby stations. It has an area of about 10 km×10 km dipping to the north-northwest direction at about 25 degree. The reflector surface is shown by iso-depth contours of thin solid lines in Fig. 1(a), and by a thick gray line in Fig. 1(b). Recently, predominant reflected P-waves (PxP phases) have been also observed in seismograms of the aftershocks of the 1998 M 5.0 earthquake (Umino *et al.*, 2001). They revealed that these PxP phases are of

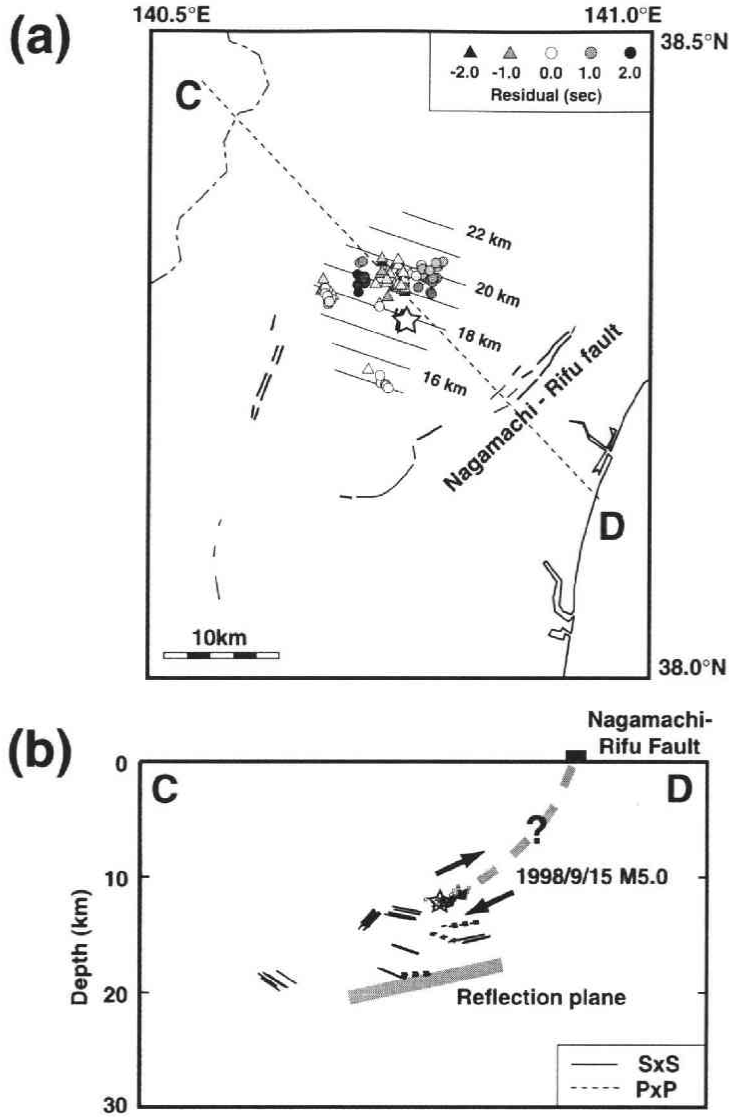

Fig. 1. Estimated S-wave reflectors beneath the focal area of 1998 M5.0 earthquake. (a) Depth distribution of a planar S-wave reflector and reflection points. Depth of the reflector is shown by contours. Circles and triangles show reflection points with positive and negative residuals of SxS-S, respectively. (b) Vertical cross section of the planar S-wave reflector and other reflectors along line C-D in (a). Thick gray line shows the planar S-wave reflector. Thin solid and broken lines show other reflectors. Surface trace of the Nagamachi-Rifu fault is shown by a thick line. Thick arrows show the fault motion of the main shock.

the same origins as was previously pointed out by Hori *et al.*, (1999).

In the 2001 seismic reflection/refraction experiments around the Nagamachi-Rifu fault, we installed a crisscross seismic array composed of off-line data recorders in order

Table 1. Locations, shot times, charge weights and P-wave velocities of 15 shot points.

Shot No	Date	Time	Latitude	Longitude	Altitude	Charge (Kg)	P-wave velocity (km/s)
1	2001, Jun. 16	01 : 01 : 00.000	38-24- 9.2934	140-31-40.9775	355.13	100	4.1
2	2001, Jun. 16	00 : 01 : 00.022	38-21-48.9578	140-38-35.0824	442.10	130	2.0
3	2001, Jun. 18	01 : 26 : 00.015	38-24-18.9763	140-44-16.1576	438.66	100	2.8
4	2001, Jun. 16	00 : 31 : 00.049	38-17-53.4700	140-37-18.2699	288.87	100	2.3
5	2001, Jun. 18	00 : 31 : 00.000	38-24-28.6487	140-47-46.9435	163.60	100	3.0
6	2001, Jun. 18	00 : 01 : 00.001	38-22-13.5097	140-47- 4.1846	159.82	100	2.3
7	2001, Jun. 16	01 : 31 : 00.039	38-19-40.5283	140-44- 2.4327	272.64	70	1.9
8	2001, Jun. 16	02 : 01 : 00.016	38-16-15.5036	140-39-54.8276	218.03	100	2.1
9	2001, Jun. 18	02 : 01 : 00.029	38-23-14.2804	140-50-33.4518	76.09	100	2.7
10	2001, Jun. 18	02 : 16 : 00.016	38-21-30.7535	140-48-46.6395	184.06	100	2.3
11	2001, Jun. 17	01 : 31 : 00.030	38-17-58.3207	140-45-37.3454	156.43	100	1.7
12	2001, Jun. 17	02 : 06 : 00.027	38-15- 4.8371	140-42-39.7932	183.50	100	2.4
13	2001, Jun. 17	00 : 01 : 00.009	38-14- 3.1535	140-48-10.6524	146.98	100	2.5
14	2001, Jun. 17	00 : 31 : 00.043	38-13-39.3738	140-45- 5.7728	131.61	100	3.3
15	2001, Jun. 17	01 : 01 : 00.055	38-12-27.7172	140-54-45.9039	3.58	100	2.3

to investigate the deep structure of the Nagamachi-Rifu fault and its relation with the fault plane of the 1998 $M5.0$ earthquake and the bright reflective layers.

2. Field observations

The seismic reflection/refraction experiments were carried out in June, 2001. Two reflection profiling receiver arrays form the backbone of the present seismic expeditions. One of the profiles, Line A, the 22-km-long NW-SE profile, is perpendicular to the surface trace of the Nagamachi-Rifu fault, and the other, Line B, the 16-km-long NE-SW profile, is parallel to the fault (Fig. 2). These two profiles are located on the hanging wall side of the Nagamachi-Rifu fault, and the Line B runs through the focal area of the 1998 $M5.0$ event. Five small-aperture seismic arrays, A1-A4 and Y1 in Fig. 2, were installed by the National Institute of Advanced Industrial Science and Technology, AIST. Five seismic arrays, 51-55 in Fig. 2, were installed in the southwestern part of the study area by Tohoku University. They are L-shaped seismic arrays by using DAT recorders. Similar L-shaped seismic arrays were installed in the Ou Backbone Range, northeastern Japan, and detected seismic scatterers and reflectors (Okada and Seismic Array Observation Group, 1998 ; Asano *et al.*, 1999). They consisted of 20 stations with a station spacing of 50 m. Details of the seismic reflection/refraction experiments were reported in Hasegawa *et al.* (2001a) and Ikawa *et al.* (2001).

Four vibrators were used for seismic wave sources. Vibration points were spaced 200 m apart on average for a total of 174 vibration points along the reflection profiling Line A and Line B. In addition to the vibrators, 70-130 kg chemical explosions were

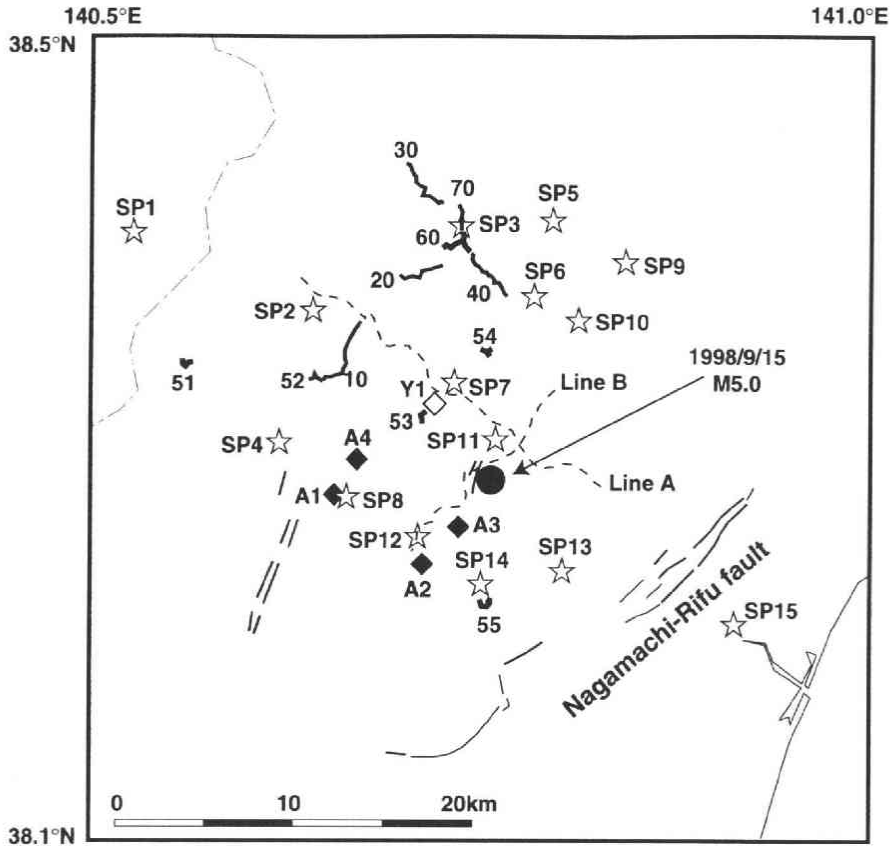

Fig. 2. Map showing locations of 2 reflection profiles, seismic arrays and 15 chemical explosions. Broken lines show the 22-km-long and 16-km-long reflection profiles (Line A and Line B). Bold lines with numerals 10-70 show the locations of crisscross seismic array with off-line data recorders. Bold lines with numerals 51-55 show the locations of L-shaped seismic arrays operated by Tohoku University. Open and solid diamonds show the locations of seismic arrays operated by GSI, AIST. Stars show the locations of 15 chemical explosions. Nagamachi-Rifu fault is indicated by thin curves.

detonated at 15 locations (SP1-15 in Fig. 2). Eight of them were placed along the reflection profiling Line A and Line B and their extensions. Others except SP15 were set up in the hanging wall side of the fault. In the previous seismic refraction surveys, shot points were usually aligned with the profiling line (*e.g.*, Research Group for Explosion Seismology, 1999a, 1999b, 1999c). In the present experiment, the locations of the chemical explosions were arranged in a 2D horizontal array in order to reveal the spatial extents of deep structure of the Nagamachi-Rifu fault and S-wave reflectors in the lower crust.

Drilling and chemical explosions were carried out by Japex Geoscience Institute Inc. (JGI). Charges were set at the bottom of the drilled holes of 14 cm diameter and 30 m

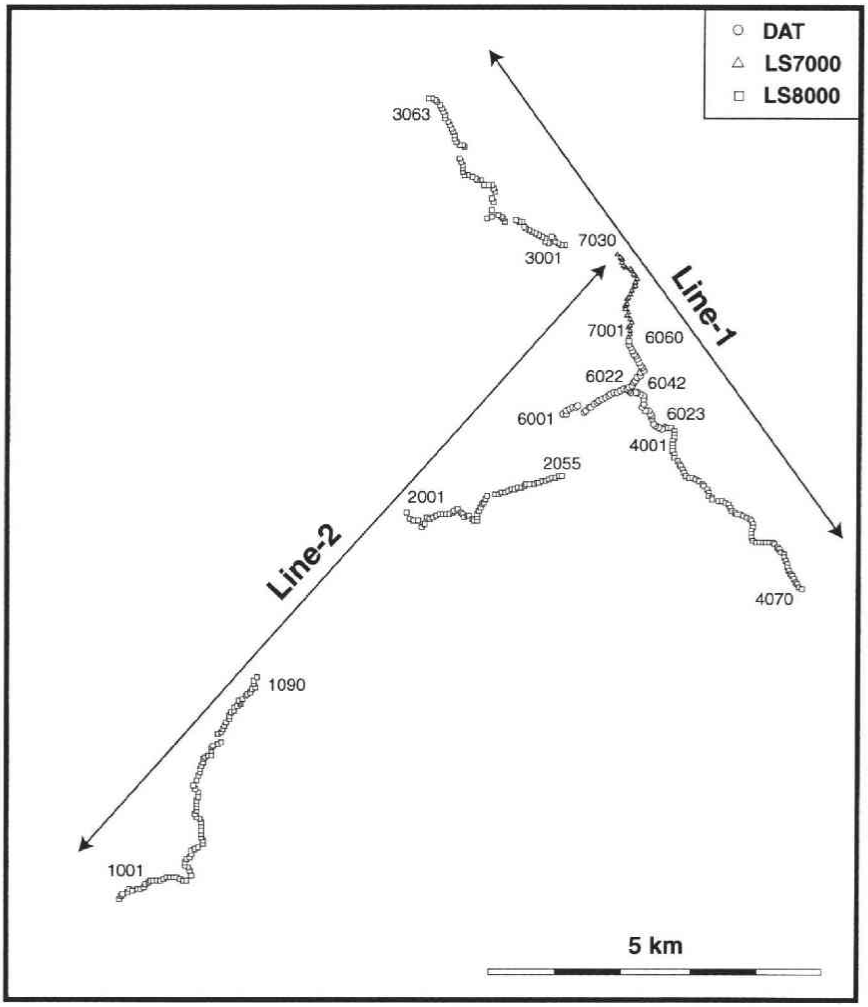

Fig. 3. Detailed map showing locations of stations for the crisscross seismic array. The locations of stations are indicated with 4-digit numbers, and are listed in Table 2.

depth, each encased with a steel pipe of 10 cm inner diameter. The height of the charge of 100 kg was about 10 m, so that the depth to the top of the charge was about 20 m. Surface P-wave velocities were determined from arrival times of P-wave recorded on 3 seismographs located very close to the drilled hole with a receiver spacing of 50 m. The result is listed in Table 1 together with shot time, location and weight of charge (data supplied by JGI).

We carried out a large seismic array observation to record these 15 shots (Research Group for Deep Structure of Nagamachi-Rifu Fault, 2001 ; Nakamura and Research Group for Deep Structure of Nagamachi-Rifu Fault, 2001). A large crisscross seismic array, composed of 368 stations with a station spacing of 50 m, was installed in the

northern part of the study area (10-70 in Fig. 2). Geophones for the seismic array were three-component or vertical-component sensors of 2 Hz (L22-D or L28-B [Mark Products Inc.]) or 4.5 Hz (L15-B [Mark Products Inc.]). Off-line data recorders (DAT recorder [Clovertech Co.], LS8000 logger or LS7000 logger [Hakusan Co.]) recorded seismic signals from the vibrators or chemical explosions at a sampling rate of 100 Hz with 16 bit or 22 bit A/D conversion. The DAT recorders and LS7000 loggers, having an ability of long-term continuous recording, recorded seismic signals from 15 chemical shots, VIBROSEIS signals and natural earthquakes. On the other hand, the LS8000 loggers worked with a event trigger system, and only recorded signals from 15 chemical shots. Locations and specifications of the seismic stations are listed in Table 2. Detailed feature of the crisscross seismic array is shown in Fig. 3. Locations of seismic stations were measured by portable Differential GPS surveys. Four crews of 8 members spent 3 days for measuring the locations of all the seismic stations by DGPS.

3. Seismic record sections

Shot gather record sections obtained by vertical-component seismometers for 15 chemical explosions, SP1-15 (Fig. 1), are shown in Fig. 4 for Line 1, and in Fig. 5 for Line 2, respectively. These waveform data are processed with a band-pass filter of 6 to 24 Hz and a 2.0-sec trailing automatic gain control correction. Discontinuity of the shot gather record section for Line 2 (Fig. 5) is due to a station gap of about 3 km between station 1090 and station 2001 (see Fig. 3).

Several predominant reflection events are observed on these shot gather record sections. Reflection events at about 5-6 sec in two-way travel-time are recognized, which are shown in Figs. 4 and 5 by solid triangles. These events correspond to the depth of the fault plane of the 1998 M5.0 earthquake (Nakamura and Research Group for Deep Structure of Nagamachi-Rifu Fault, 2001). Reflection events at about 6-7 sec in two-way travel-time are recognized, and are shown in Figs. 4 and 5 by solid circles. These events correspond to the depth of the S-wave reflector in the lower crust (Hori *et al.*, 1999). Reflection events at about 3-5 sec and about 8 sec in two-way travel-time are recognized, and are shown in Figs. 4 and 5 by open triangles and circles, respectively. Moreover, reflection events at about 10 sec in two-way travel-time are sometimes recognized. They correspond to the depth of the Moho discontinuity (Hasegawa *et al.*, 2001a). It is hoped that future precise analyses of those records will clarify the deep structure of the Nagamachi-Rifu fault and the structure of the S-wave reflecting surfaces (bright spots).

4. Conclusion

Seismic experiments were carried out for the purpose of clarifying the deep structure of the Nagamachi-Rifu fault. Well-developed late Cenozoic calderas are distributed in the major part of the study area (Yoshida, 2001), and the geological structure is

Table 2. Locations, type of recorders and seismographs of seismic stations.

Station No.	Latitude (N)	Longitude(E)	Alititude(m)	Recorder	Seismograph	Component
1001	38.32938	140.65074	335	LS8000	L-22D	1
1002	38.32984	140.65107	330	LS8000	L-22D	1
1003	38.33006	140.65140	325	LS8000	L-22D	1
1004	38.33034	140.65207	325	LS8000	L-22D	1
1005	38.33064	140.65247	325	LS8000	L-22D	1
1006	38.33056	140.65305	325	LS8000	L-22D	1
1007	38.33064	140.65377	325	LS8000	L-22D	1
1008	38.33081	140.65449	325	LS8000	L-22D	1
1009	38.33099	140.65490	325	LS8000	L-22D	1
1010	38.33129	140.65525	325	LS8000	L-22D	1
1011	38.33161	140.65572	325	LS8000	L-22D	1
1012	38.33174	140.65625	325	LS8000	L-22D	1
1013	38.33187	140.65684	325	LS8000	L-22D	1
1014	38.33186	140.65729	325	LS8000	L-22D	1
1015	38.33174	140.65792	320	LS8000	L-22D	1
1016	38.33206	140.65832	315	LS8000	L-22D	1
1017	38.33216	140.65889	310	LS8000	L-22D	1
1018	38.33217	140.65945	310	LS8000	L-22D	1
1019	38.33219	140.66020	310	LS8000	L-22D	1
1020	38.33218	140.66079	310	LS8000	L-22D	1
1021	38.33205	140.66124	305	LS8000	L-22D	1
1022	38.33190	140.66180	300	LS8000	L-22D	1
1023	38.33177	140.66239	300	LS8000	L-22D	1
1024	38.33257	140.66317	325	LS8000	L-22D	1
1025	38.33306	140.66295	330	LS8000	L-22D	1
1026	38.33353	140.66256	335	LS8000	L-22D	1
1027	38.33389	140.66218	340	LS8000	L-22D	1
1028	38.33432	140.66207	340	LS8000	L-22D	1
1029	38.33479	140.66238	350	LS8000	L-22D	1
1030	38.33483	140.66288	360	LS8000	L-22D	1
1031	38.33543	140.66316	370	LS8000	L-22D	1
1032	38.33590	140.66315	360	LS8000	L-22D	1
1033	38.33606	140.66371	350	LS8000	L-22D	1
1034	38.33638	140.66431	345	LS8000	L-22D	1
1035	38.33680	140.66521	340	LS8000	L-22D	1
1036	38.33723	140.66520	340	LS8000	L-22D	1
1037	38.33760	140.66494	340	LS8000	L-22D	1
1038	38.33810	140.66487	340	LS8000	L-22D	1
1039	38.33860	140.66480	340	LS8000	L-22D	1
1040	38.33910	140.66487	345	LS8000	L-22D	1
1041	38.33959	140.66477	345	LS8000	L-22D	1
1042	38.34002	140.66447	350	LS8000	L-22D	1
1043	38.34031	140.66400	355	LS8000	L-22D	1
1044	38.34063	140.66383	360	LS8000	L-22D	1
1045	38.34109	140.66393	355	LS8000	L-22D	1
1046	38.34151	140.66415	360	LS8000	L-22D	1
1047	38.34204	140.66411	360	LS8000	L-22D	1
1048	38.34257	140.66416	360	LS8000	L-22D	1
1049	38.34294	140.66424	360	LS8000	L-22D	1
1050	38.34357	140.66421	360	LS8000	L-22D	1
1051	38.34412	140.66372	365	LS8000	L-22D	1
1052	38.34448	140.66348	370	LS8000	L-22D	1
1053	38.34507	140.66401	405	LS8000	L-22D	1

Table 2. continued

Station No.	Latitude (N)	Longitude(E)	Alititude(m)	Recorder	Seismograph	Component
1054	38.34588	140.66431	410	LS8000	L-22D	1
1055	38.34631	140.66456	410	LS8000	L-22D	1
1056	38.34673	140.66473	420	LS8000	L-22D	1
1057	38.34711	140.66486	425	LS8000	L-22D	1
1058	38.34754	140.66525	425	LS8000	L-22D	1
1059	38.34798	140.66512	430	LS8000	L-22D	1
1060	38.34829	140.66540	435	LS8000	L-22D	1
1061	38.34848	140.66603	440	LS8000	L-22D	1
1062	38.34851	140.66658	450	LS8000	L-22D	1
1063	38.34909	140.66648	450	LS8000	L 22D	1
1064	38.34954	140.66654	450	LS8000	L-22D	1
1065	38.34984	140.66699	450	LS8000	L-22D	1
1066	38.34995	140.66758	455	LS8000	L-22D	1
1067	38.35037	140.66815	455	LS8000	L-22D	1
1068	38.35131	140.66768	435	LS8000	L-22D	1
1069	38.35161	140.66815	425	LS8000	L-22D	1
1070	38.35200	140.66844	420	LS8000	L-22D	1
1071	38.35253	140.66879	415	LS8000	L-22D	1
1072	38.35298	140.66920	405	LS8000	L-22D	1
1073	38.35344	140.66956	400	LS8000	L-22D	1
1074	38.35374	140.66974	395	LS8000	L-22D	1
1075	38.35417	140.67006	395	LS8000	L-22D	1
1076	38.35460	140.67044	390	LS8000	L-22D	1
1077	38.35496	140.67054	385	LS8000	L-22D	1
1078	38.35510	140.67109	380	LS8000	L-22D	1
1079	38.35532	140.67165	375	LS8000	L-22D	1
1080	38.35561	140.67180	375	LS8000	L-22D	1
1081	38.35592	140.67152	365	LS8000	L-22D	1
1082	38.35615	140.67192	365	LS8000	L-22D	1
1083	38.35654	140.67243	365	LS8000	L-22D	1
1084	38.35675	140.67276	365	LS8000	L-22D	1
1085	38.35704	140.67324	360	LS8000	L-22D	1
1086	38.35740	140.67367	355	LS8000	L-22D	1
1087	38.35768	140.67410	355	LS8000	L-22D	1
1088	38.35812	140.67395	355	LS8000	L-22D	1
1089	38.35844	140.67396	348	LS8000	L-22D	1
1090	38.35889	140.67459	343	LS8000	L-22D	1
2001	38.38091	140.69967	540	LS8000	L-22D	1
2002	38.37997	140.70024	515	LS8000	L-22D	1
2003	38.37986	140.70084	505	LS8000	L-22D	1
2004	38.37982	140.70165	505	LS8000	L-22D	1
2005	38.37899	140.70212	495	LS8000	L-22D	1
2006	38.37936	140.70267	500	LS8000	L-22D	1
2007	38.38017	140.70307	500	LS8000	L-22D	1
2008	38.38009	140.70362	495	LS8000	L-22D	1
2009	38.38028	140.70420	495	LS8000	L-22D	1
2010	38.38051	140.70464	500	LS8000	L-22D	1
2011	38.38074	140.70515	495	LS8000	L-22D	1
2012	38.38069	140.70577	495	LS8000	L-22D	1
2013	38.38067	140.70632	495	LS8000	L-22D	1
2014	38.38079	140.70689	495	LS8000	L-22D	1
2015	38.38099	140.70740	495	LS8000	L-22D	1
2016	38.38126	140.70780	495	LS8000	L-22D	1

Table 2. continued

Station No.	Latitude (N)	Longitude(E)	Alititude(m)	Recorder	Seismograph	Component
2017	38.38134	140.70837	495	LS8000	L-22D	1
2018	38.38099	140.70879	490	LS8000	L-22D	1
2019	38.38067	140.70910	490	LS8000	L-22D	1
2020	38.38027	140.70942	490	LS8000	L-22D	1
2021	38.38059	140.70992	495	LS8000	L-22D	1
2022	38.38046	140.71044	495	LS8000	L-22D	1
2023	38.38016	140.71085	495	LS8000	L-22D	1
2024	38.37986	140.71125	495	LS8000	L-22D	1
2025	38.37989	140.71170	500	LS8000	L-22D	1
2026	38.38036	140.71170	510	LS8000	L-22D	1
2027	38.38079	140.71177	515	LS8000	L-22D	1
2028	38.38122	140.71200	515	LS8000	L-22D	1
2029	38.38159	140.71237	510	LS8000	L-22D	1
2030	38.38196	140.71265	510	LS8000	L-22D	1
2031	38.38226	140.71299	510	LS8000	L-22D	1
2032	38.38269	140.71315	510	LS8000	L 22D	1
2033	38.38306	140.71355	510	LS8000	L-22D	1
2034	38.38331	140.71484	530	LS8000	L-22D	1
2035	38.38344	140.71540	530	LS8000	L-22D	1
2036	38.38353	140.71600	530	LS8000	L-22D	1
2037	38.38366	140.71655	530	LS8000	L-22D	1
2038	38.38386	140.71705	530	LS8000	L-22D	1
2039	38.38397	140.71757	530	LS8000	L-22D	1
2040	38.38407	140.71819	530	LS8000	L-22D	1
2041	38.38419	140.71870	530	LS8000	L-22D	1
2042	38.38429	140.71925	530	LS8000	L-22D	1
2043	38.38439	140.71984	525	LS8000	L-22D	1
2044	38.38464	140.72032	520	LS8000	L-22D	1
2045	38.38469	140.72090	510	LS8000	L-22D	1
2046	38.38477	140.72150	510	LS8000	L-22D	1
2047	38.38487	140.72205	510	LS8000	L-22D	1
2048	38.38500	140.72254	510	LS8000	L-22D	1
2049	38.38515	140.72309	510	LS8000	L-22D	1
2050	38.38526	140.72362	505	LS8000	L-22D	1
2051	38.38539	140.72412	505	LS8000	L-22D	1
2052	38.38552	140.72473	505	LS8000	L-22D	1
2053	38.38563	140.72525	505	LS8000	L-22D	1
2054	38.38575	140.72583	505	LS8000	L-22D	1
2055	38.38586	140.72638	505	LS8000	L-22D	1
3001	38.41664	140.72678	670	LS8000	L-22D	1
3002	38.41677	140.72610	675	LS8000	L-22D	1
3003	38.41691	140.72545	680	LS8000	L-22D	1
3004	38.41722	140.72496	685	LS8000	L-22D	1
3005	38.41757	140.72465	690	LS8000	L-22D	1
3006	38.41776	140.72440	690	LS8000	L-22D	1
3007	38.41696	140.72385	705	LS8000	L-22D	1
3008	38.41724	140.72326	715	LS8000	L-22D	1
3009	38.41767	140.72318	720	LS8000	L-22D	1
3010	38.41791	140.72271	725	LS8000	L-22D	1
3011	38.41809	140.72220	730	LS8000	L-22D	1
3012	38.41832	140.72165	730	LS8000	L-22D	1
3013	38.41852	140.72111	735	LS8000	L-22D	1
3014	38.41867	140.72061	740	LS8000	L-22D	1

Table 2. continued

Station No.	Latitude (N)	Longitude(E)	Alititude(m)	Recorder	Seismograph	Component
3015	38.41887	140.72005	745	LS8000	L-22D	1
3016	38.41911	140.71956	750	LS8000	L-22D	1
3017	38.41972	140.71931	755	LS8000	L-22D	1
3018	38.41983	140.71875	760	LS8000	L-22D	1
3019	38.42009	140.71825	765	LS8000	L-22D	1
3020	38.41991	140.71635	785	LS8000	L-22D	1
3021	38.42024	140.71605	785	LS8000	L-22D	1
3022	38.42056	140.71566	790	LS8000	L-22D	1
3023	38.42064	140.71516	795	LS8000	L-22D	1
3024	38.42037	140.71393	800	LS8000	L-22D	1
3025	38.42031	140.71313	810	LS8000	L-22D	1
3026	38.42144	140.71388	820	LS8000	L-22D	1
3027	38.42239	140.71438	825	LS8000	L-22D	1
3028	38.42291	140.71413	830	LS8000	L-22D	1
3029	38.42382	140.71458	830	LS8000	L-22D	1
3030	38.42421	140.71433	830	LS8000	L-22D	1
3031	38.42461	140.71393	835	LS8000	L-22D	1
3032	38.42464	140.71331	835	LS8000	L-22D	1
3033	38.42477	140.71245	835	LS8000	L-22D	1
3034	38.42530	140.71208	830	LS8000	L-22D	1
3035	38.42544	140.71159	830	LS8000	L-22D	1
3036	38.42566	140.71108	825	LS8000	L-22D	1
3037	38.42584	140.71060	825	LS8000	L-22D	1
3038	38.42601	140.70985	820	LS8000	L-22D	1
3039	38.42601	140.70918	815	LS8000	L-22D	1
3040	38.42641	140.70893	810	LS8000	L-22D	1
3041	38.42687	140.70893	805	LS8000	L-22D	1
3042	38.42734	140.70880	805	LS8000	L-22D	1
3043	38.42781	140.70871	805	LS8000	L-22D	1
3044	38.42824	140.70846	800	LS8000	L-22D	1
3045	38.42975	140.70931	805	LS8000	L-22D	1
3046	38.42995	140.70880	810	LS8000	L-22D	1
3047	38.43010	140.70822	810	LS8000	L-22D	1
3048	38.43050	140.70786	810	LS8000	L-22D	1
3049	38.43090	140.70758	810	LS8000	L-22D	1
3050	38.43135	140.70740	815	LS8000	L-22D	1
3051	38.43182	140.70715	815	LS8000	L-22D	1
3052	38.43233	140.70696	810	LS8000	L-22D	1
3053	38.43268	140.70658	810	LS8000	L-22D	1
3054	38.43317	140.70633	805	LS8000	L-22D	1
3055	38.43350	140.70580	800	LS8000	L-22D	1
3056	38.43402	140.70570	800	LS8000	L-22D	1
3057	38.43452	140.70561	795	LS8000	L-22D	1
3058	38.43497	140.70529	795	LS8000	L-22D	1
3059	38.43538	140.70495	790	LS8000	L-22D	1
3060	38.43578	140.70453	785	LS8000	L-22D	1
3061	38.43612	140.70413	785	LS8000	L-22D	1
3062	38.43622	140.70358	780	LS8000	L-22D	1
3063	38.43627	140.70285	775	LS8000	L-22D	1
4001	38.39217	140.74456	370	LS8000	L-22D	1
4002	38.39219	140.74516	365	LS8000	L-22D	1
4003	38.39186	140.74560	365	LS8000	L-22D	1
4004	38.39139	140.74568	360	LS8000	L-22D	1

Table 2. continued

Station No.	Latitude (N)	Longitude(E)	Alititude(m)	Recorder	Seismograph	Component
4005	38.39091	140.74560	355	LS8000	L-22D	1
4006	38.39046	140.74540	350	LS8000	L-22D	1
4007	38.38999	140.74533	350	LS8000	L-22D	1
4008	38.38954	140.74526	345	LS8000	L-22D	1
4009	38.38914	140.74540	340	LS8000	L-22D	1
4010	38.38867	140.74548	340	LS8000	L-22D	1
4011	38.38824	140.74568	335	LS8000	L-22D	1
4012	38.38784	140.74606	335	LS8000	L-22D	1
4013	38.38747	140.74643	330	LS8000	L-22D	1
4014	38.38707	140.74666	330	LS8000	L-22D	1
4015	38.38669	140.74710	325	LS8000	L-22D	1
4016	38.38621	140.74720	320	LS8000	L-22D	1
4017	38.38584	140.74760	315	LS8000	L-22D	1
4018	38.38571	140.74823	310	LS8000	L-22D	1
4019	38.38551	140.74873	305	LS8000	L-22D	1
4020	38.38531	140.74923	300	LS8000	L-22D	1
4021	38.38507	140.74979	300	LS8000	L-22D	1
4022	38.38482	140.75035	295	LS8000	L-22D	1
4023	38.38446	140.75076	295	LS8000	L-22D	1
4024	38.38406	140.75111	290	LS8000	L-22D	1
4025	38.38359	140.75140	290	LS8000	L-22D	1
4026	38.38324	140.75165	285	LS8000	L-22D	1
4027	38.38292	140.75211	280	LS8000	L-22D	1
4028	38.38272	140.75223	280	LS8000	L-22D	1
4029	38.38249	140.75331	275	LS8000	L-22D	1
4030	38.38251	140.75386	270	LS8000	L-22D	1
4031	38.38232	140.75438	265	LS8000	L-22D	1
4032	38.38204	140.75490	265	LS8000	L-22D	1
4033	38.38162	140.75518	265	LS8000	L-22D	1
4034	38.38121	140.75543	265	LS8000	L-22D	1
4035	38.38104	140.75591	265	LS8000	L-22D	1
4036	38.38082	140.75641	265	LS8000	L-22D	1
4037	38.38064	140.75696	265	LS8000	L-22D	1
4038	38.38046	140.75746	265	LS8000	L-22D	1
4039	38.38031	140.75800	265	LS8000	L 22D	1
4040	38.38016	140.75851	260	LS8000	L-22D	1
4041	38.37977	140.75881	260	LS8000	L-22D	1
4042	38.37936	140.75905	255	LS8000	L-22D	1
4043	38.37891	140.75908	255	LS8000	L-22D	1
4044	38.37852	140.75883	250	LS8000	L-22D	1
4045	38.37812	140.75891	245	LS8000	L-22D	1
4046	38.37762	140.75895	240	LS8000	L-22D	1
4047	38.37724	140.75920	235	LS8000	L-22D	1
4048	38.37697	140.75966	235	LS8000	L-22D	1
4049	38.37686	140.76023	230	LS8000	L-22D	1
4050	38.37687	140.76080	225	LS8000	L-22D	1
4051	38.37692	140.76145	220	LS8000	L-22D	1
4052	38.37694	140.76195	220	LS8000	L-22D	1
4053	38.37696	140.76251	215	LS8000	L-22D	1
4054	38.37672	140.76293	210	LS8000	L-22D	1
4055	38.37636	140.76333	210	LS8000	L-22D	1
4056	38.37602	140.76366	205	LS8000	L-22D	1
4057	38.37567	140.76405	205	LS8000	L-22D	1

Table 2. continued

Station No.	Latitude (N)	Longitude(E)	Alititude(m)	Recorder	Seismograph	Component
4058	38.37529	140.76438	200	LS8000	L-22D	1
4059	38.37489	140.76463	200	LS8000	L-22D	1
4060	38.37451	140.76491	200	LS8000	L-22D	1
4061	38.37406	140.76513	200	LS8000	L-22D	1
4062	38.37361	140.76520	200	LS8000	L-22D	1
4063	38.37319	140.76528	195	LS8000	L-22D	1
4064	38.37281	140.76551	195	LS8000	L-22D	1
4065	38.37244	140.76586	195	LS8000	L-22D	1
4066	38.37207	140.76621	195	LS8000	L-22D	1
4067	38.37167	140.76653	190	LS8000	L-22D	1
4068	38.37129	140.76683	190	LS8000	L-22D	1
4069	38.37094	140.76716	190	LS8000	L-22D	1
4070	38.37061	140.76756	190	LS8000	L-22D	1
6001	38.39419	140.72653	580	DAT	L-28B	3
6002	38.39432	140.72706	575	DAT	L-28B	3
6003	38.39461	140.72729	750	DAT	L-28B	3
6004	38.39484	140.72767	560	DAT	L-28B	3
6005	38.39517	140.72825	550	DAT	L-28B	3
6006	38.39504	140.72875	545	DAT	L-28B	3
6007	38.39525	140.72926	535	DAT	L-28B	3
6008	38.39443	140.73026	510	DAT	L-28B	3
6009	38.39472	140.73069	505	DAT	L-28B	3
6010	38.39501	140.73119	500	DAT	L-28B	3
6011	38.39519	140.73154	495	DAT	L-28B	3
6012	38.39551	140.73204	490	DAT	L-28B	3
6013	38.39573	140.73251	485	DAT	L-28B	3
6014	38.39598	140.73297	485	DAT	L-28B	3
6015	38.39620	140.73336	480	DAT	L-28B	3
6016	38.39647	140.73387	480	DAT	L-28B	3
6017	38.39668	140.73444	470	DAT	L-28B	3
6018	38.39693	140.73468	465	DAT	L-28B	3
6019	38.39707	140.73531	455	DAT	L-28B	3
6020	38.39719	140.73585	450	DAT	L-28B	3
6021	38.39733	140.73644	440	DAT	L-28B	3
6022	38.39746	140.73694	435	DAT	L-28B	3
6023	38.39240	140.74404	365	DAT	L-28B	3
6024	38.39218	140.74354	370	DAT	L-28B	3
6025	38.39246	140.74292	370	DAT	L-28B	3
6026	38.39269	140.74250	375	DAT	L-28B	3
6027	38.39298	140.74216	380	DAT	L-28B	3
6028	38.39351	140.74200	385	DAT	L-28B	3
6029	38.39388	140.74179	390	DAT	L-28B	3
6030	38.39432	140.74161	390	DAT	L-28B	3
6031	38.39456	140.74119	395	DAT	L-28B	3
6032	38.39472	140.74068	395	DAT	L-28B	3
6033	38.39517	140.74020	400	DAT	L-28B	3
6034	38.39565	140.74038	405	DAT	L-28B	3
6035	38.39611	140.74033	410	DAT	L-28B	3
6036	38.39659	140.74033	410	DAT	L-28B	3
6037	38.39689	140.73997	415	DAT	L-28B	3
6038	38.39709	140.73945	420	DAT	L-28B	3
6039	38.39710	140.73895	420	DAT	L-28B	3
6040	38.39704	140.73817	425	DAT	L-28B	3

Table 2. continued

Station No.	Latitude (N)	Longitude(E)	Alititude(m)	Recorder	Seismograph	Component
6041	38.39728	140.73784	425	DAT	L-28B	3
6042	38.39762	140.73754	425	DAT	L-28B	3
6043	38.39778	140.73801	420	DAT	L-28B	3
6044	38.39798	140.73847	420	DAT	L-28B	3
6045	38.39839	140.73890	415	DAT	L-28B	3
6046	38.39875	140.73895	415	DAT	L-28B	3
6047	38.39912	140.73936	415	DAT	L-28B	3
6048	38.39939	140.73977	410	DAT	L-28B	3
6049	38.39984	140.73996	410	DAT	L-28B	3
6050	38.40006	140.74046	405	DAT	L-28B	3
6051	38.40039	140.74028	405	DAT	L-28B	3
6052	38.40073	140.73996	410	DAT	L-28B	3
6053	38.40119	140.73969	410	DAT	L-28B	3
6054	38.40156	140.73940	415	DAT	L-28B	3
6055	38.40192	140.73904	415	DAT	L-28B	3
6056	38.40224	140.73865	420	DAT	L-28B	3
6057	38.40261	140.73835	420	DAT	L-28B	3
6058	38.40305	140.73810	425	DAT	L-28B	3
6059	38.40343	140.73786	430	DAT	L-28B	3
6060	38.40389	140.73789	435	DAT	L-28B	3
7001	38.40438	140.73787	435	LS7000	L-22D	3
7002	38.40474	140.73794	435	LS7000	L-22D	3
7003	38.40527	140.73795	435	LS7000	L-22D	3
7004	38.40566	140.73781	440	LS7000	L-22D	3
7005	38.40603	140.73796	440	LS7000	L-22D	3
7006	38.40640	140.73822	445	LS7000	L-22D	3
7007	38.40685	140.73808	450	LS7000	L-22D	3
7008	38.40721	140.73763	455	LS7000	L-22D	3
7009	38.40775	140.73775	455	LS7000	L-22D	3
7010	38.40809	140.73732	460	LS7000	L-22D	3
7011	38.40853	140.73733	465	LS7000	L-22D	3
7012	38.40894	140.73747	470	LS7000	L-22D	3
7013	38.40942	140.73750	475	LS7000	L-22D	3
7014	38.40976	140.73782	475	LS7000	L-22D	3
7015	38.41019	140.73805	480	LS7000	L-22D	3
7016	38.41065	140.73826	485	LS7000	L-22D	3
7017	38.41099	140.73858	490	LS7000	L-22D	3
7018	38.41134	140.73901	495	LS7000	L-22D	3
7019	38.41179	140.73901	500	LS7000	L-22D	3
7020	38.41213	140.73913	500	LS7000	L-22D	3
7021	38.41259	140.73898	505	LS7000	L-22D	3
7022	38.41291	140.73869	510	LS7000	L-22D	3
7023	38.41335	140.73824	510	LS7000	L-22D	3
7024	38.41360	140.73793	515	LS7000	L-22D	3
7025	38.41367	140.73712	520	LS7000	L-22D	3
7026	38.41400	140.73684	525	LS7000	L-22D	3
7027	38.41436	140.73657	530	LS7000	L-22D	3
7028	38.41477	140.73660	530	LS7000	L-22D	3
7029	38.41517	140.73624	535	LS7000	L-22D	3
7030	38.41542	140.73589	535	LS7000	L-22D	3

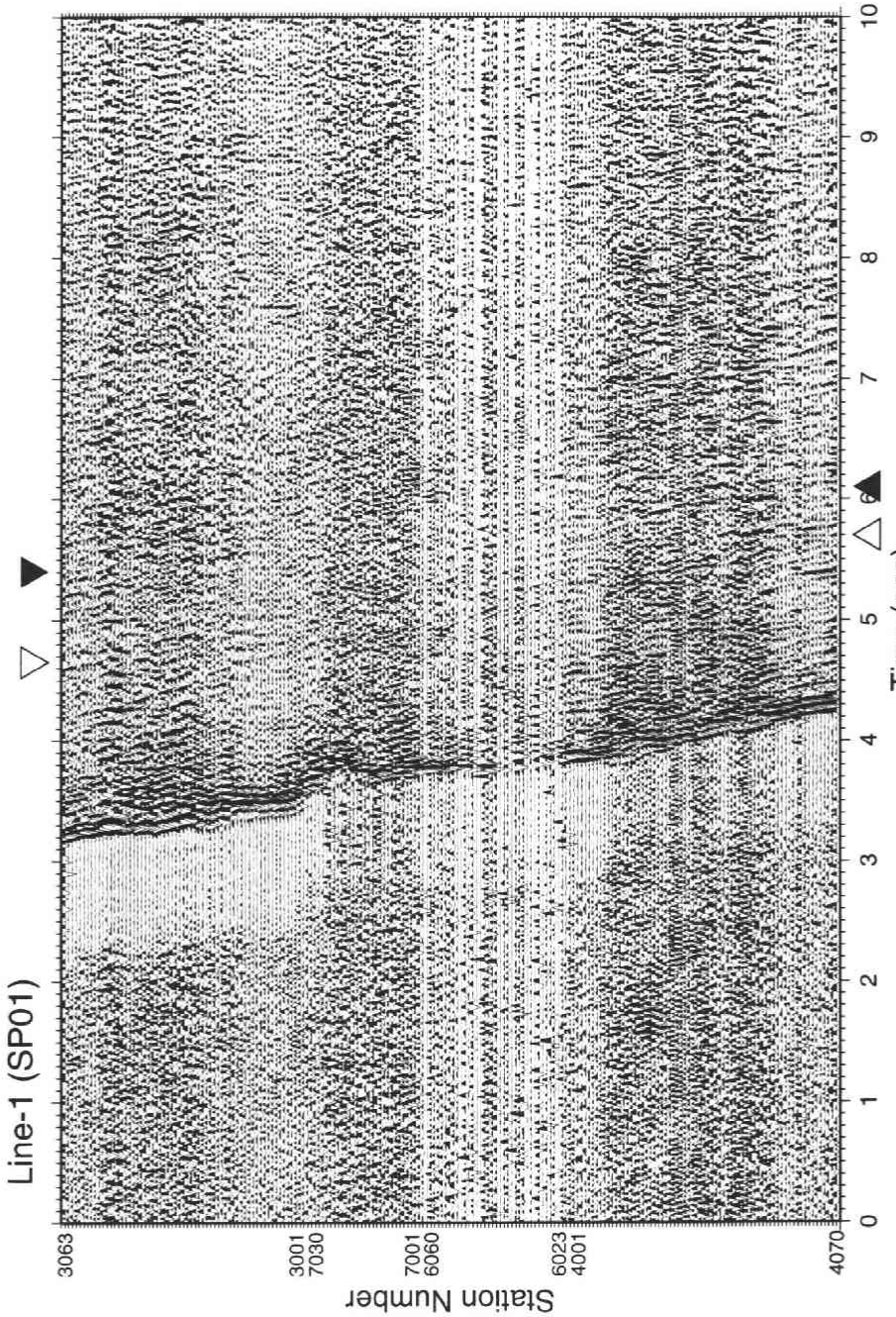

Fig. 4(a). Shot gather record sections along Line 1. Vertical-component record sections from SP1.

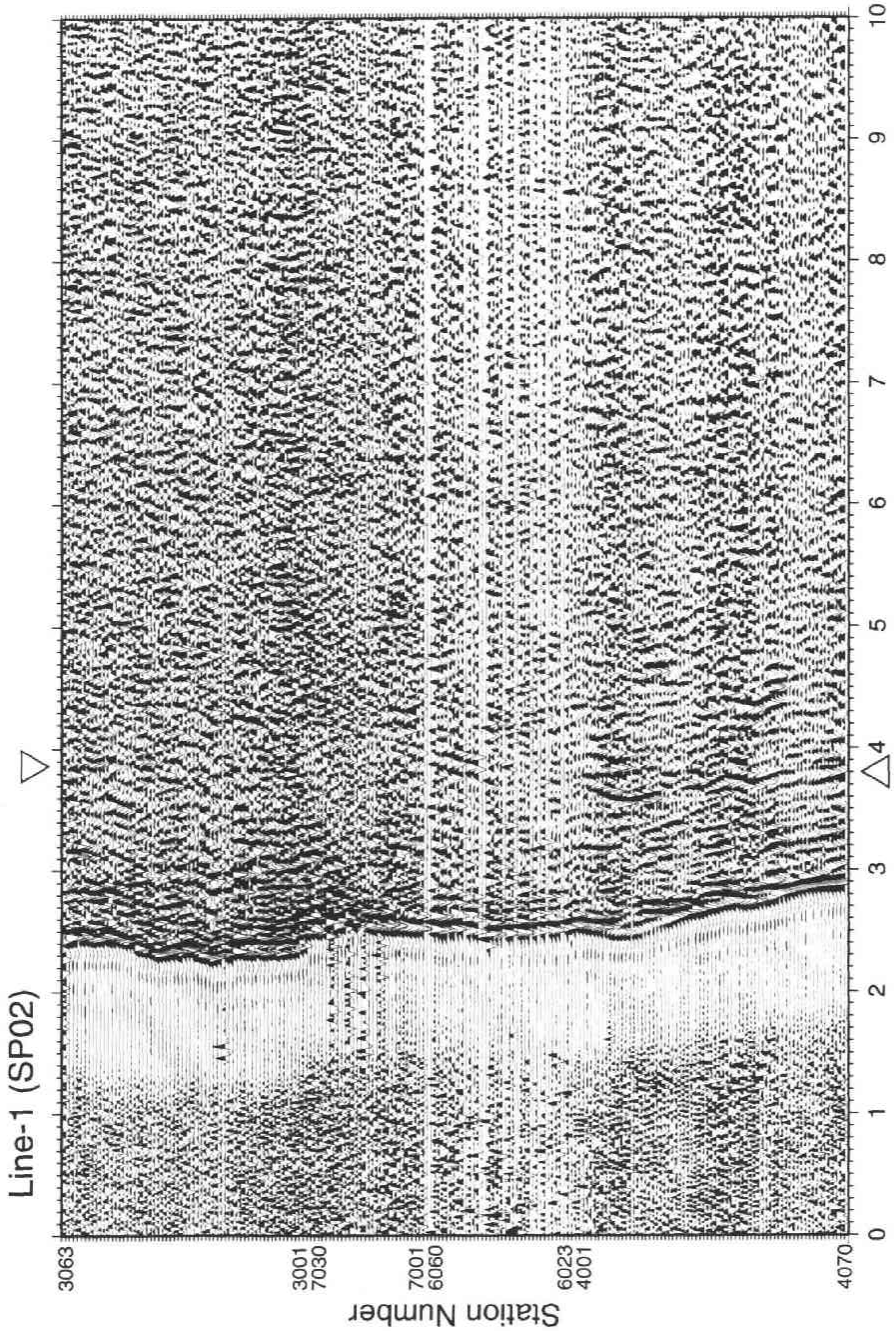

Fig. 4(b). Shot gather record sections along Line 1. Vertical-component record sections from SP2.

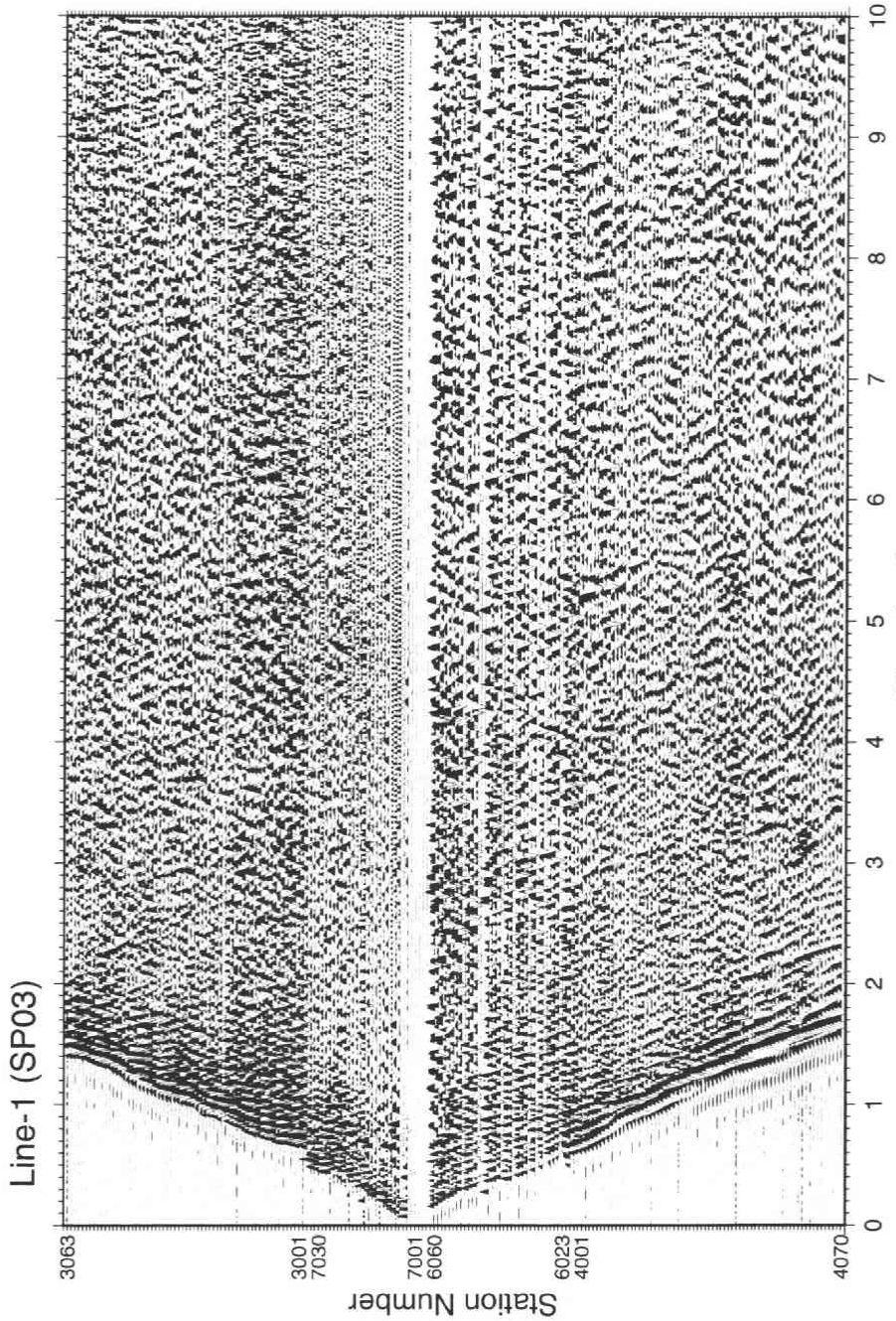

Fig. 4(c). Shot gather record sections along Line 1. Vertical component record sections from SP3.

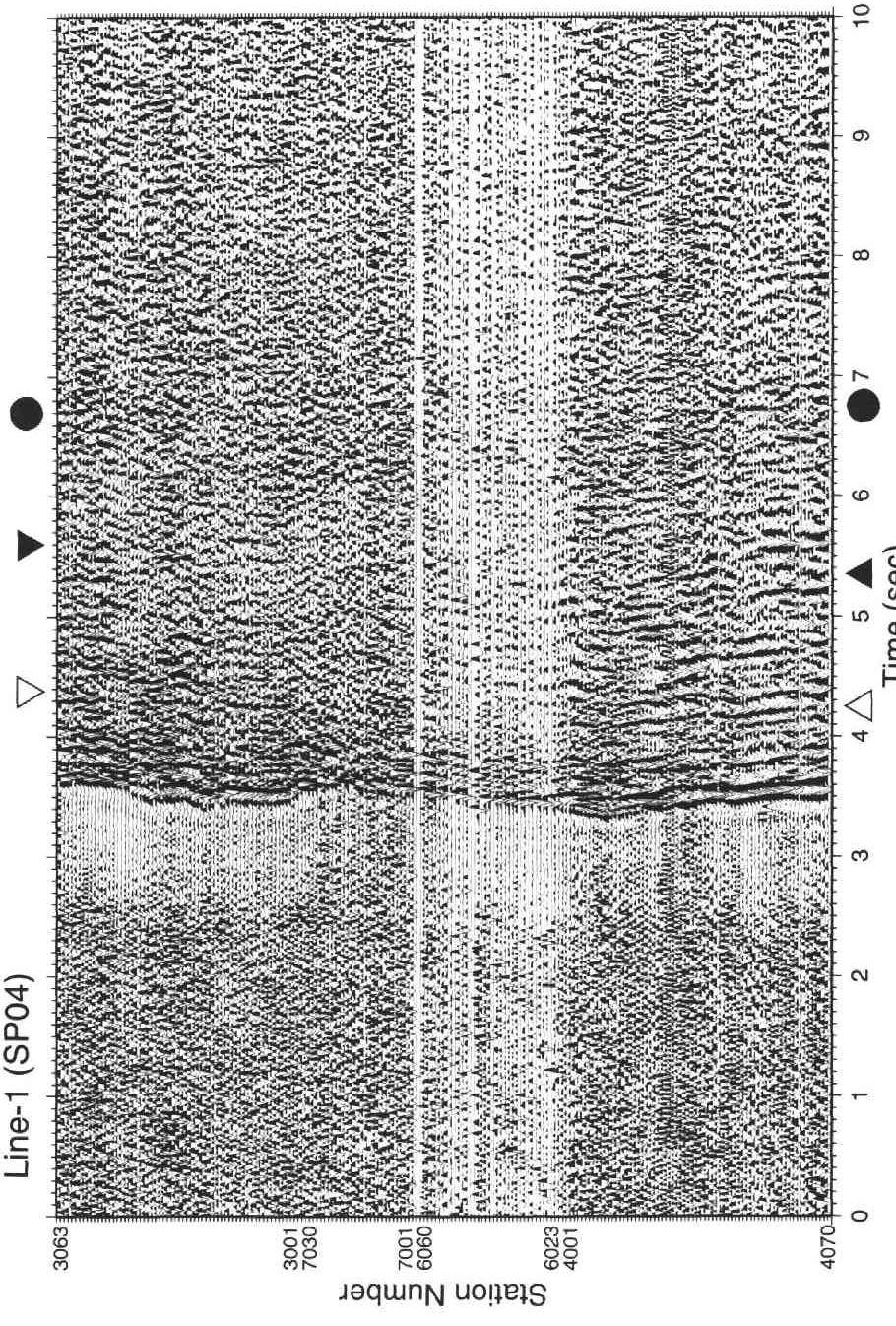

Fig. 4(d). Shot gather record sections along Line 1. Vertical-component record sections from SP4.

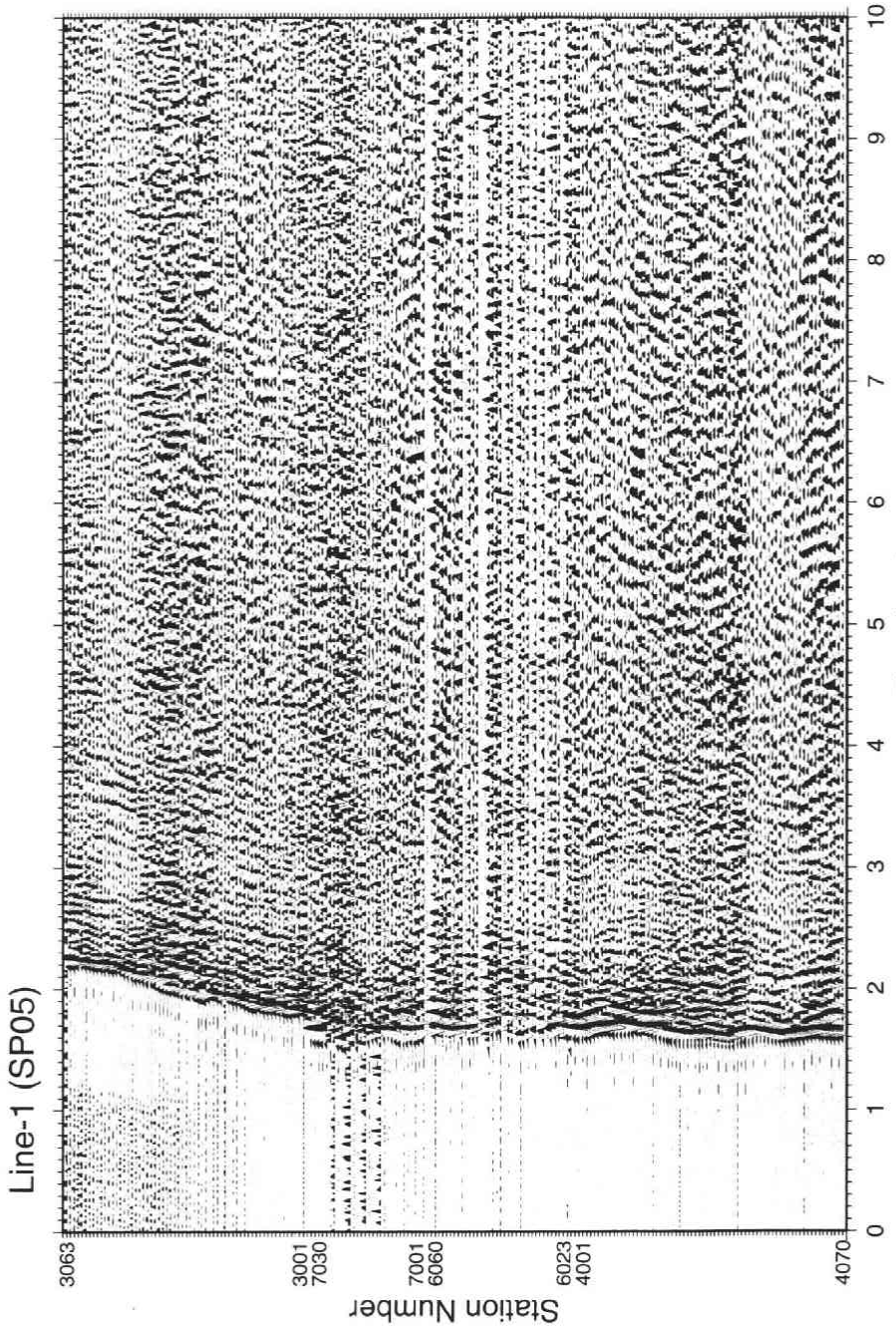

Fig. 4(e). Shot gather record sections along Line 1. Vertical-component record sections from SP5.

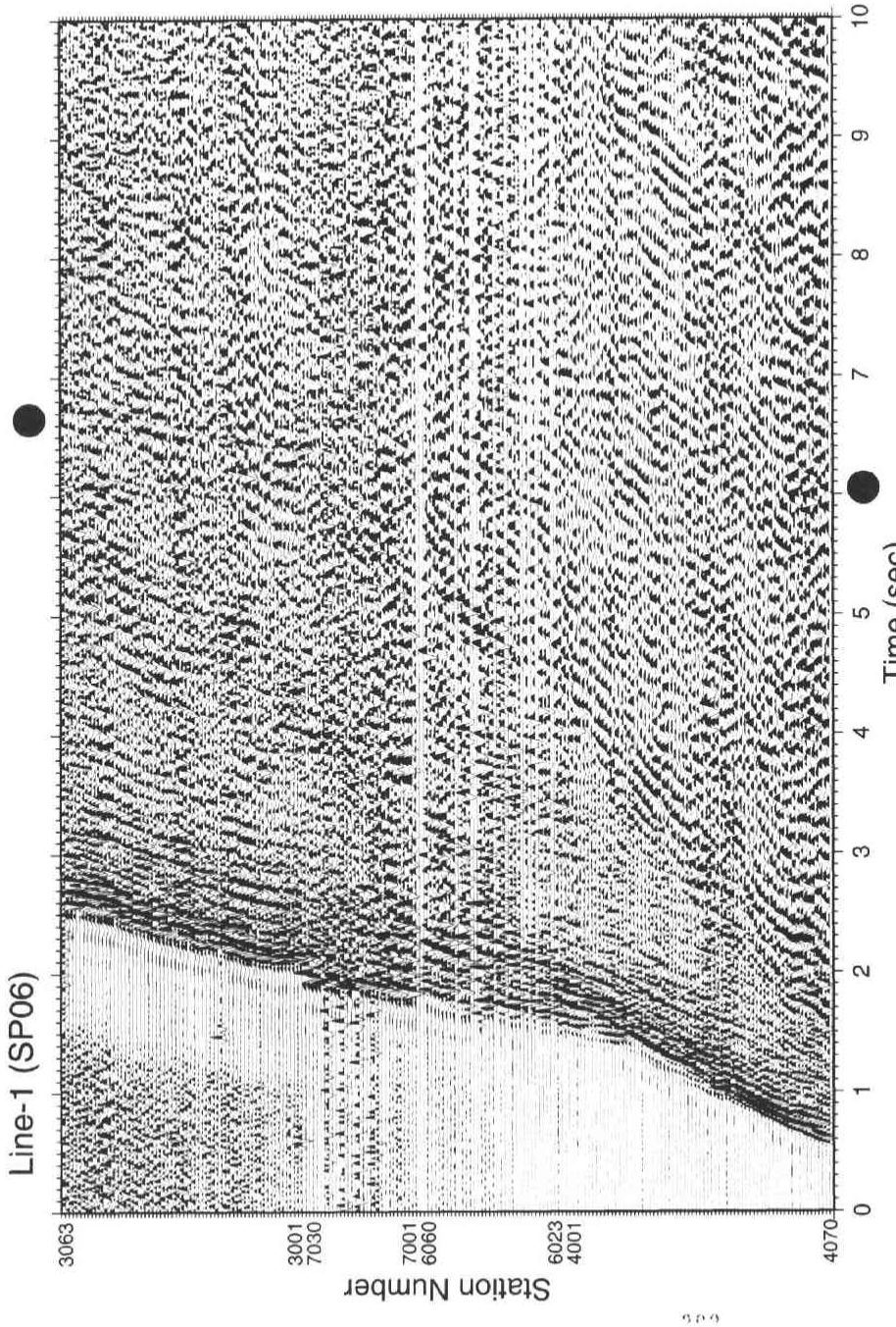

Fig. 4(f). Shot gather record sections along Line 1. Vertical-component record sections from SP6.

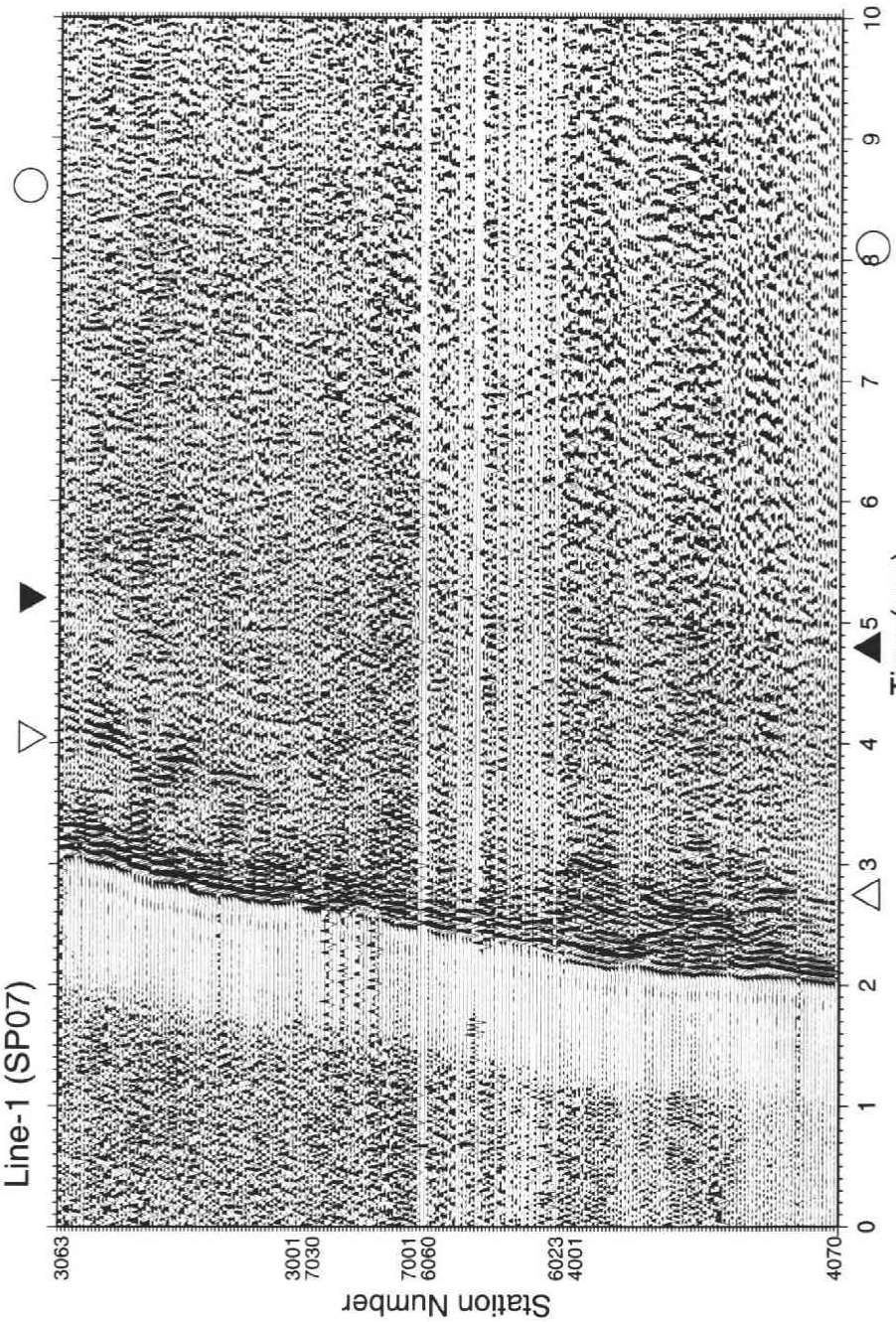

Fig. 4(g). Shot gather record sections along Line 1. Vertical-component record sections from SP7.

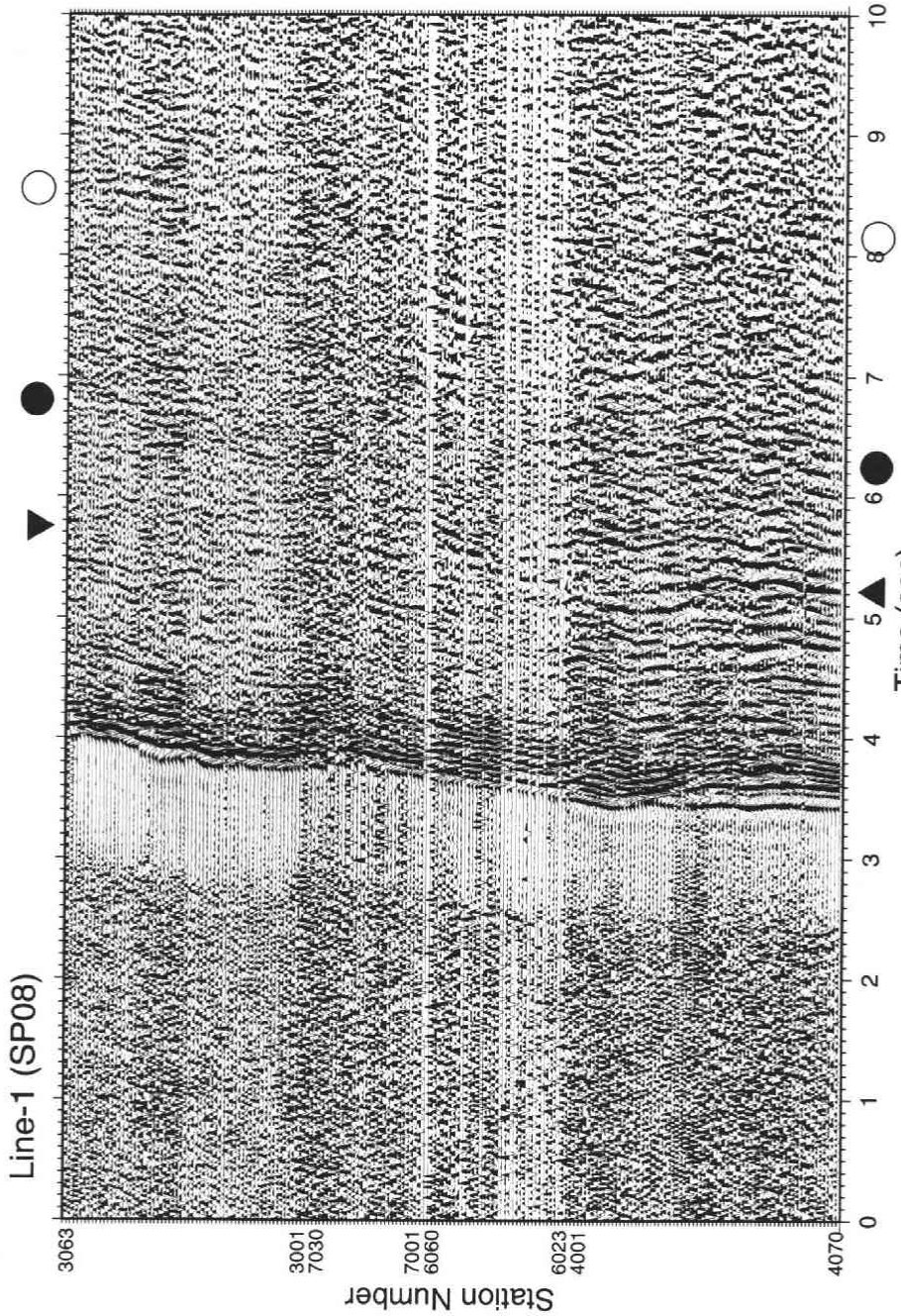

Fig. 4(h). Shot gather record sections along Line 1. Vertical-component record sections from SP8.

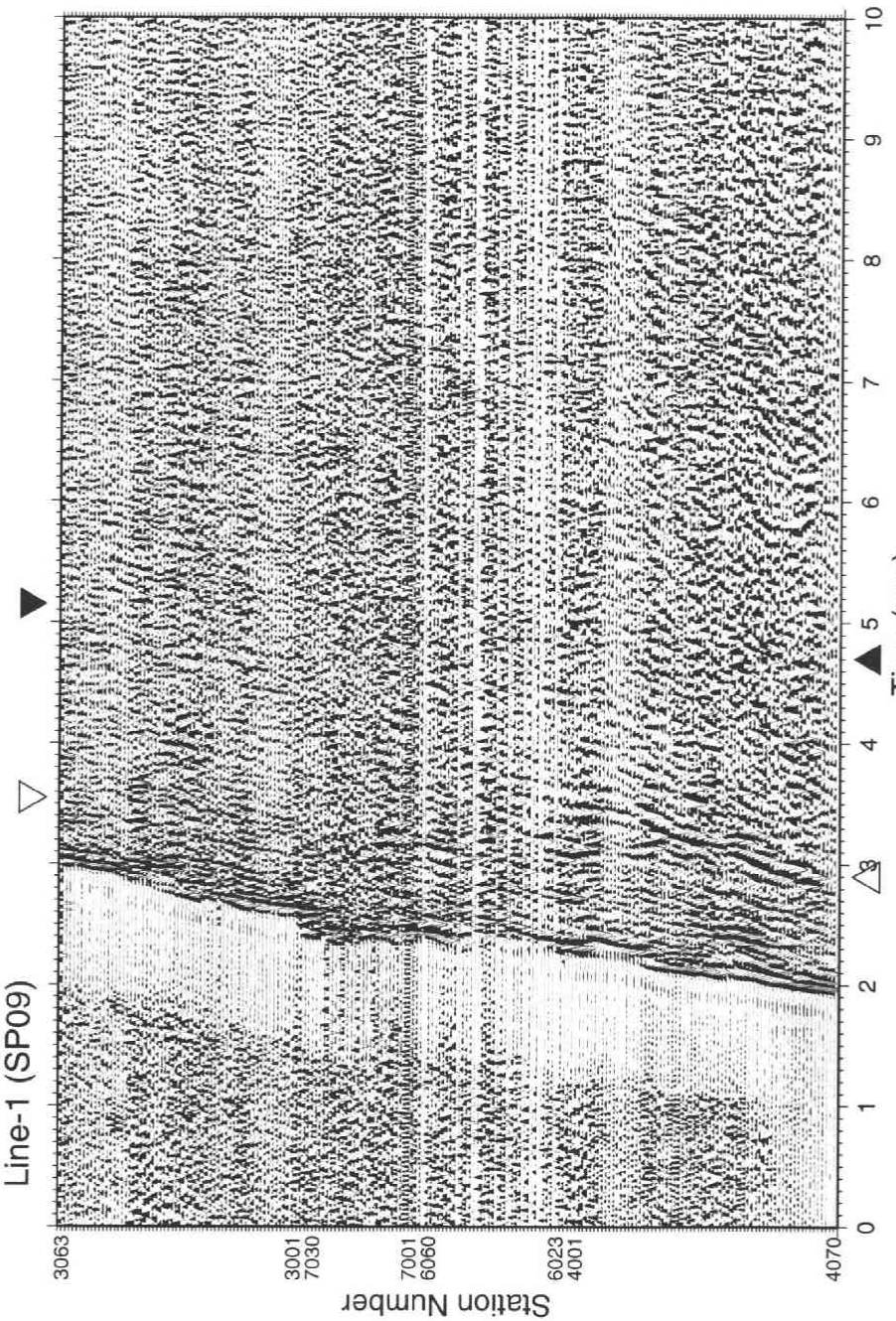

Fig. 4(i). Shot gather record sections along Line 1. Vertical component record sections from SP9.

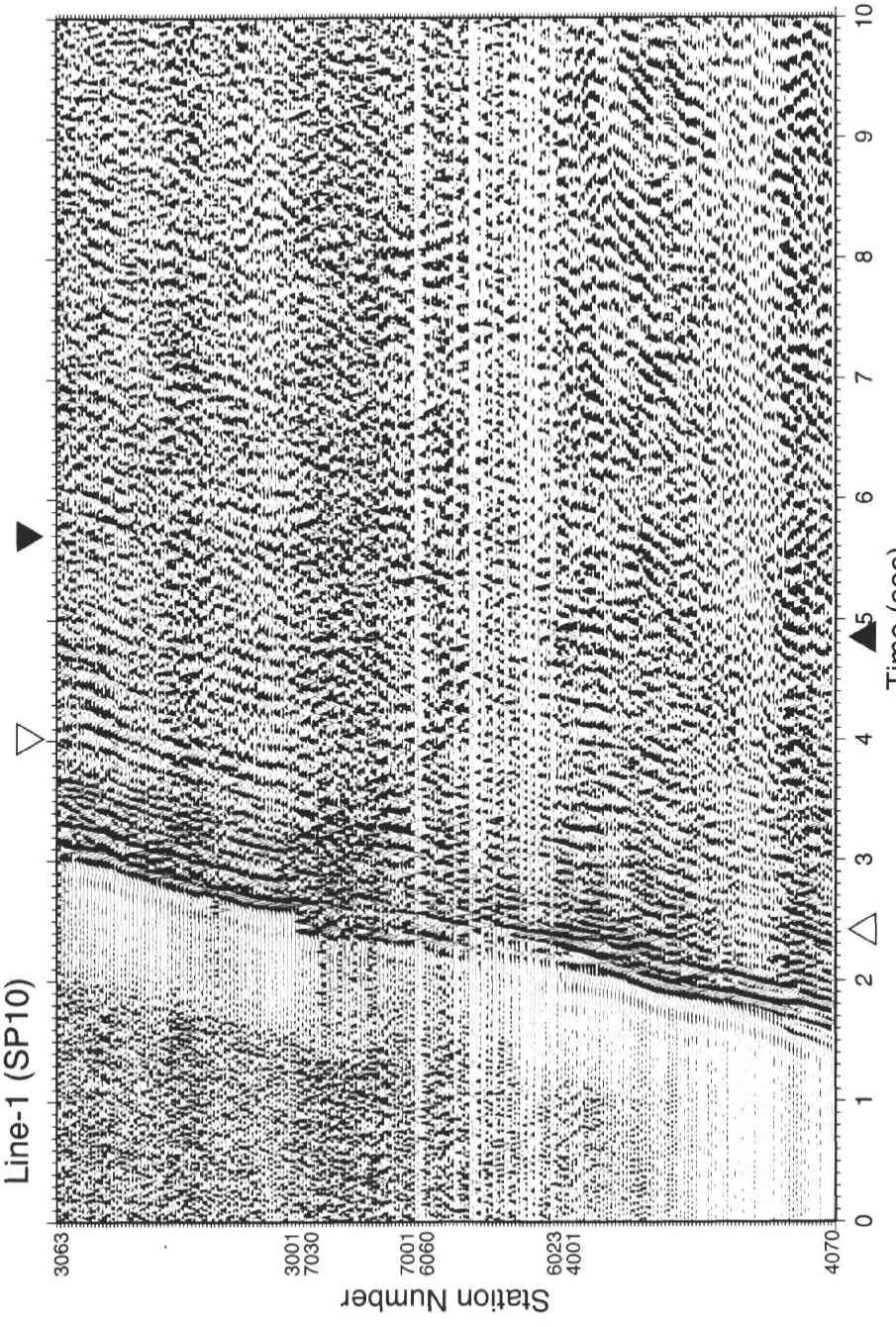

Fig. 4(j). Shot gather record sections along Line 1. Vertical-component record sections from SP10.

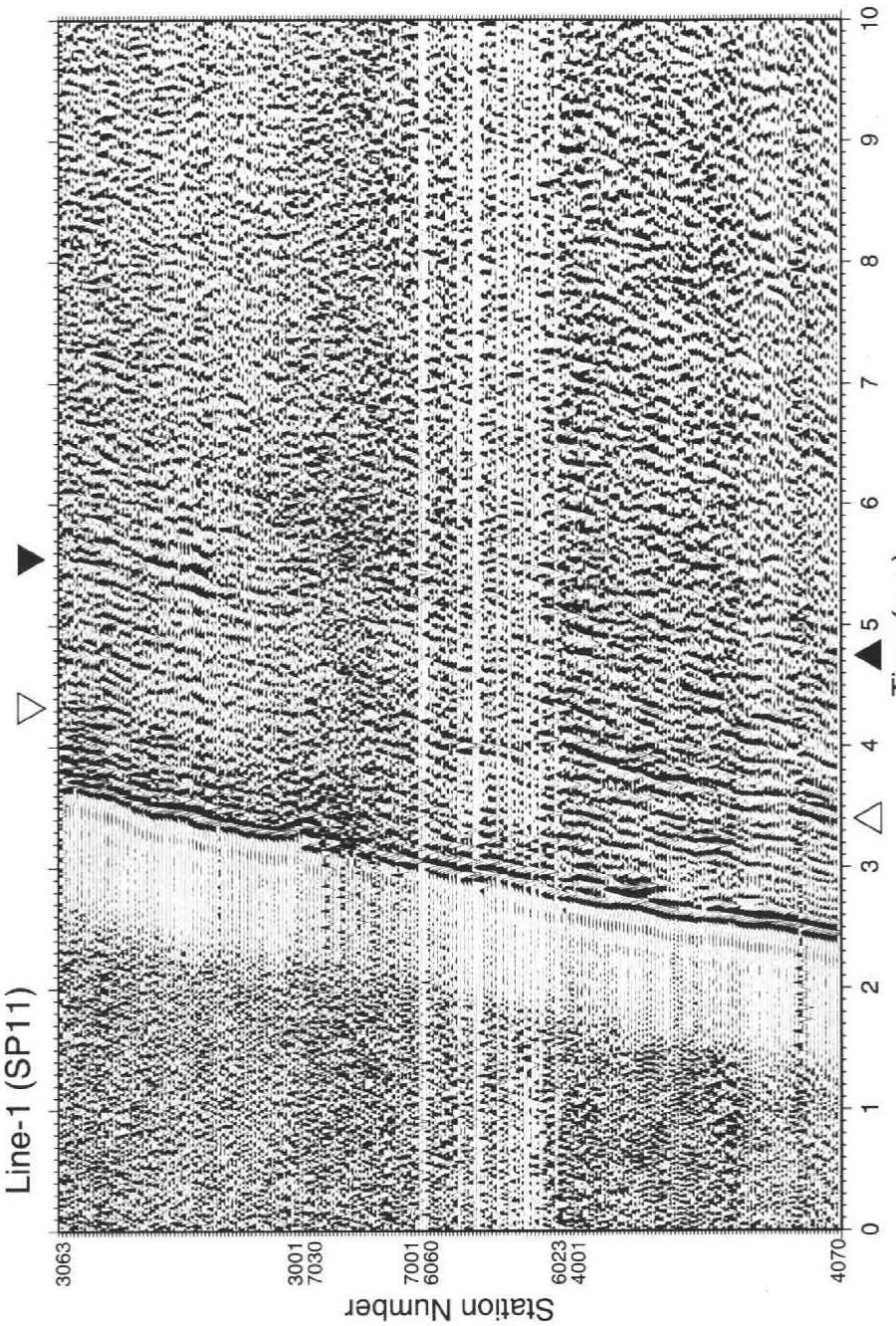

Fig. 4(k). Shot gather record sections along Line 1. Vertical-component record sections from SP11.

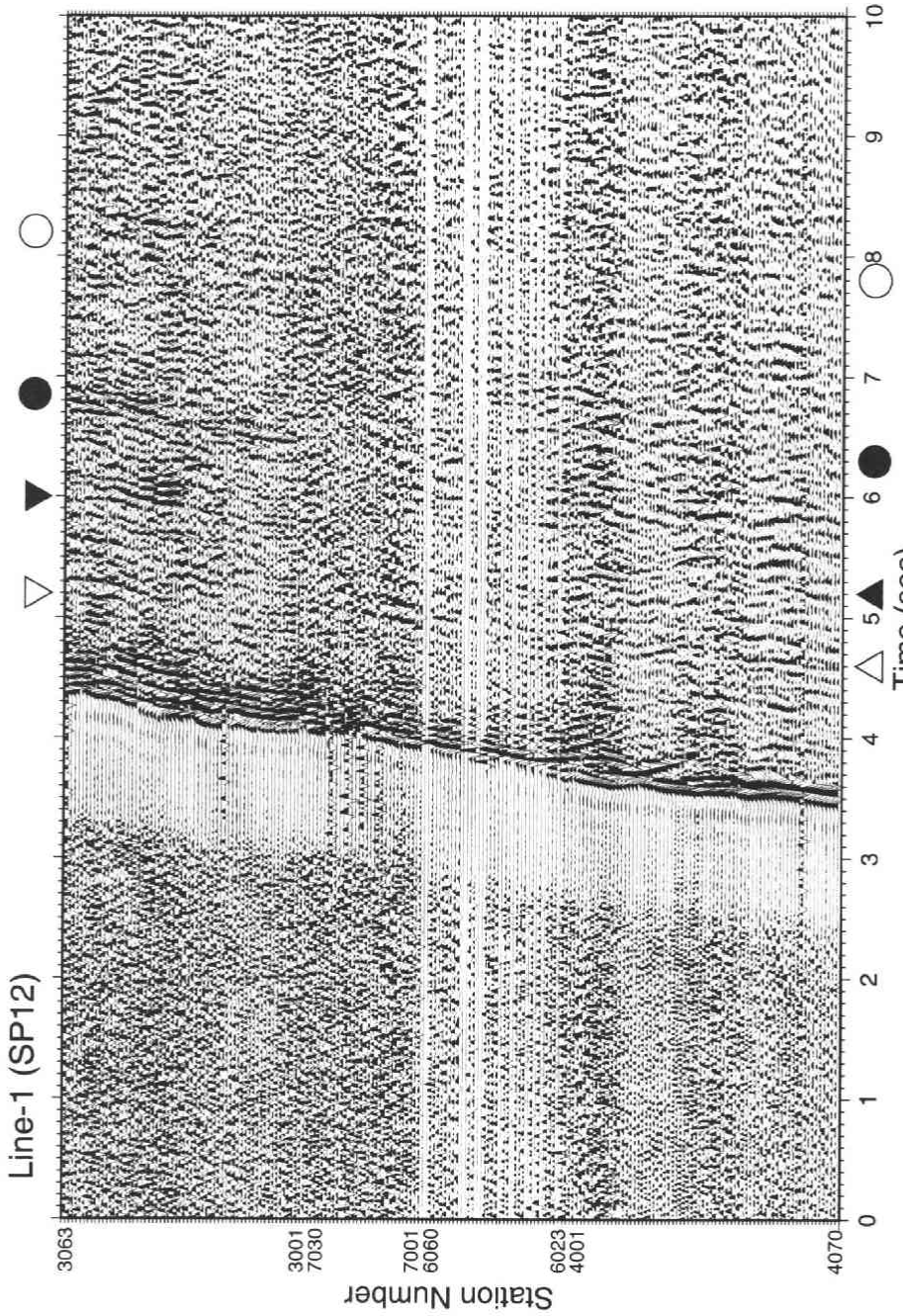

Fig. 4(b). Shot gather record sections along Line 1. Vertical-component record sections from SP12.

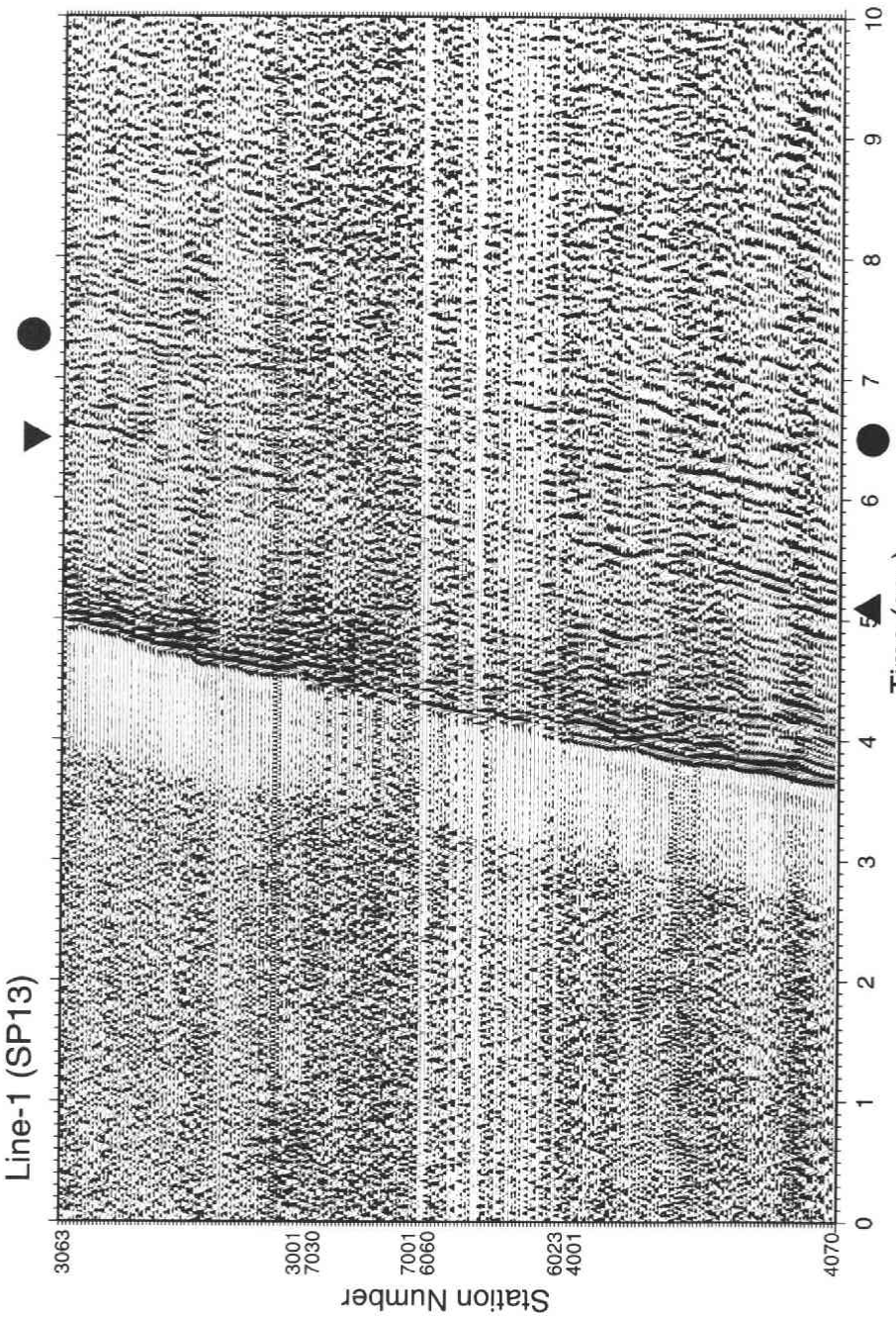

Fig. 4(m). Shot gather record sections along Line 1. Vertical-component record sections from SP13.

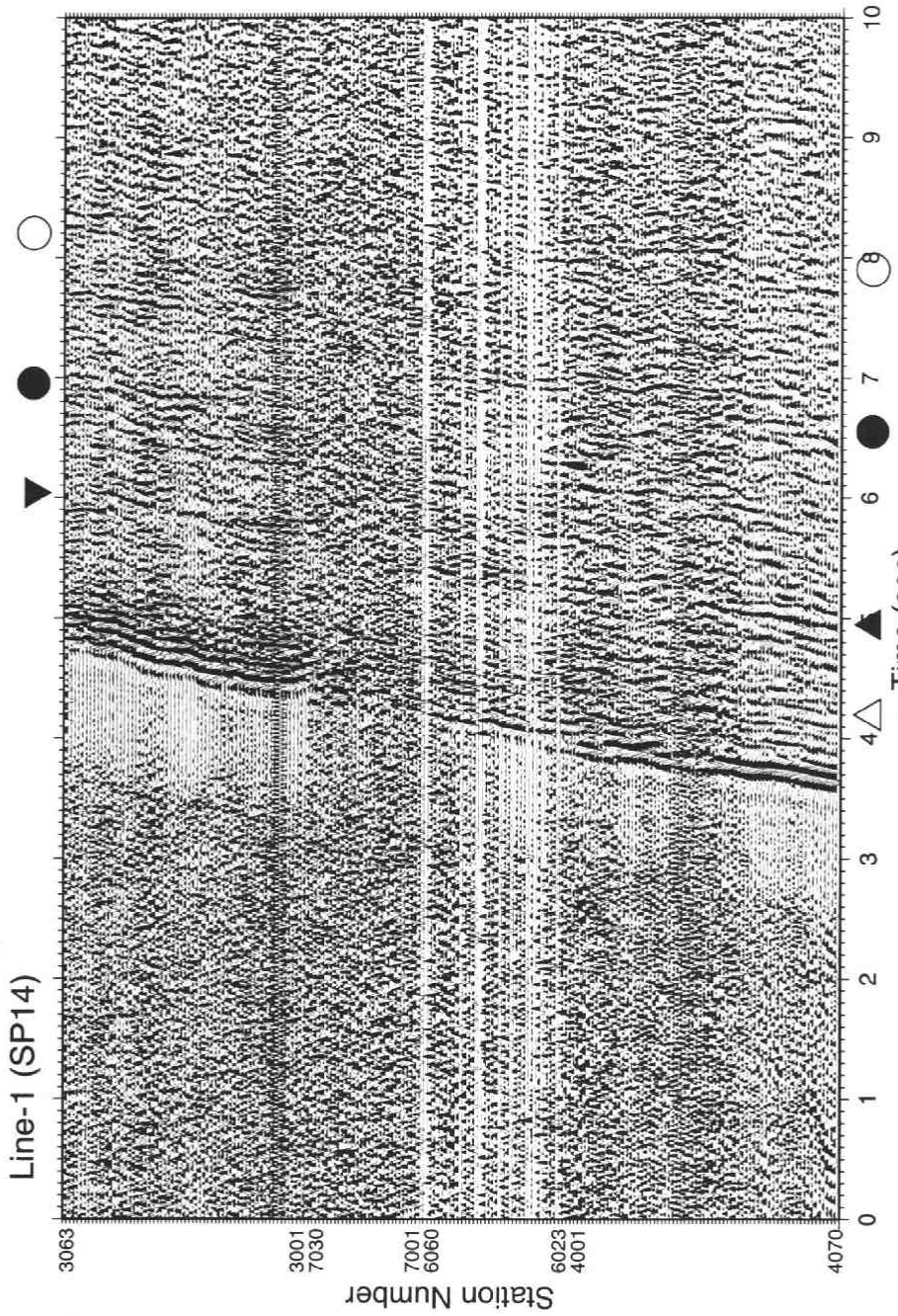

Fig. 4(n). Shot gather record sections along Line 1. Vertical-component record sections from SP14.

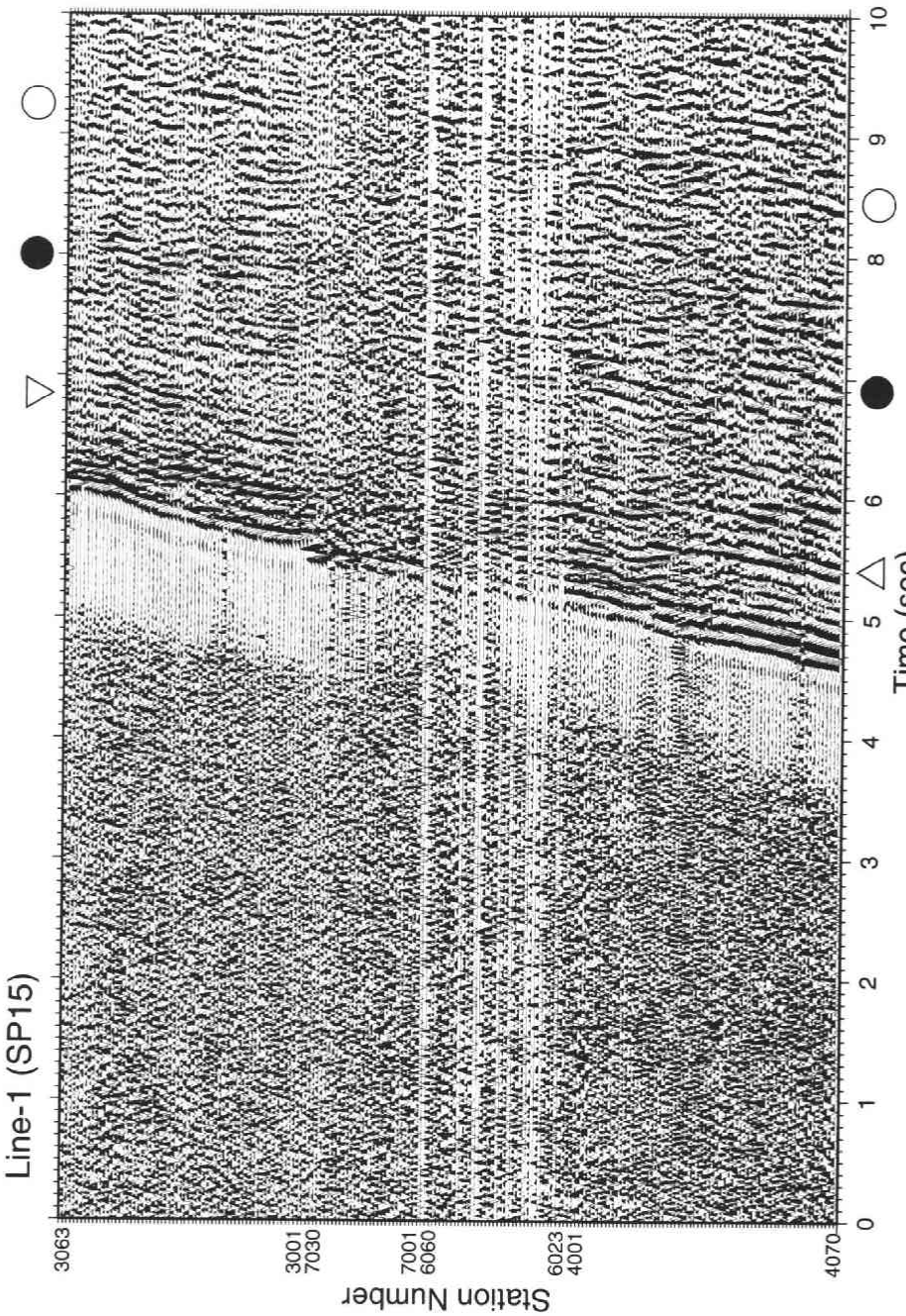

Fig. 4(a). Shot gather record sections along Line 1. Vertical-component record sections from SP15.

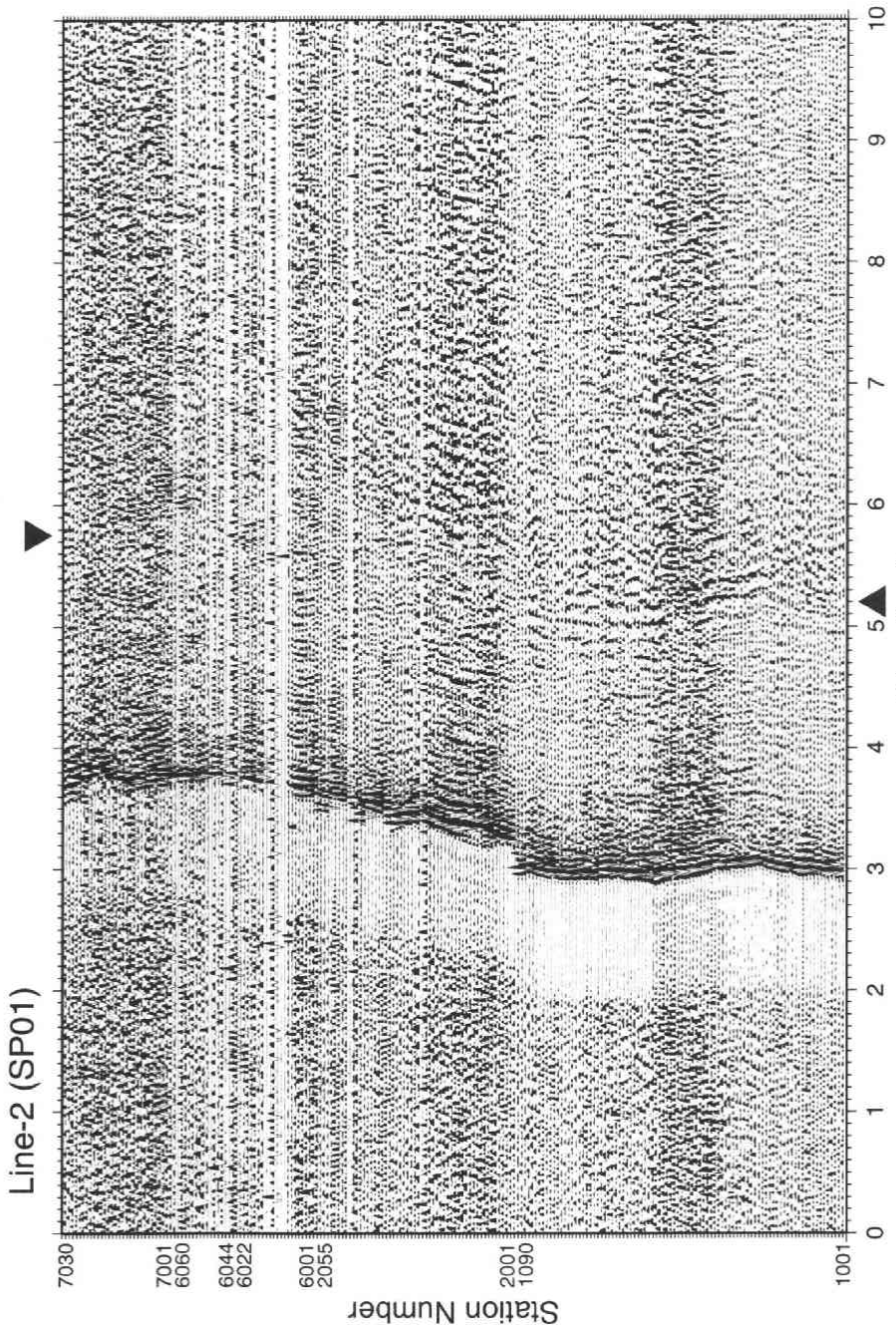

Fig. 5(a). Shot gather record sections along Line 2. Vertical-component record sections from SP1.

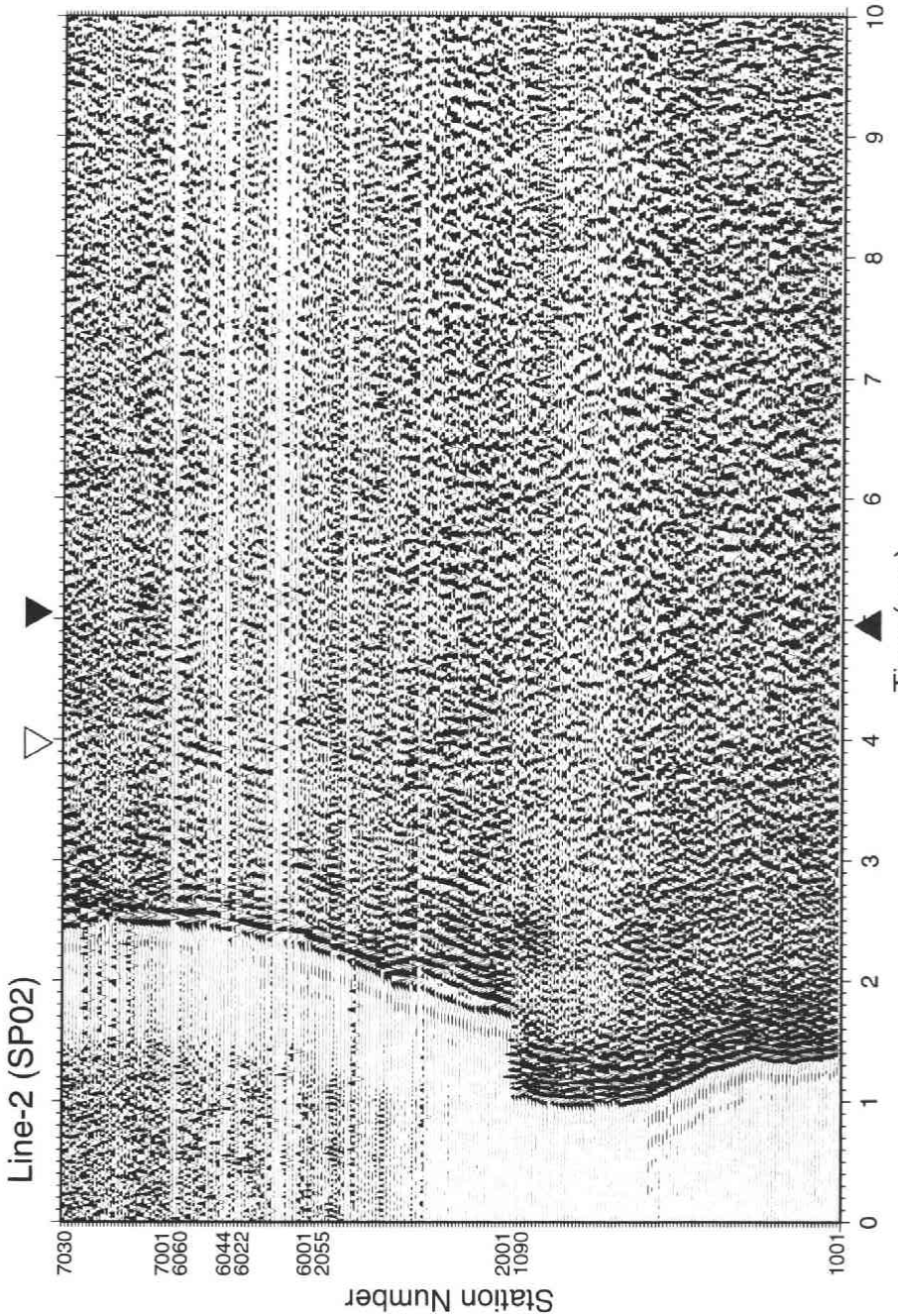

Fig. 5(b). Shot gather record sections along Line 2. Vertical-component record sections from SP2.

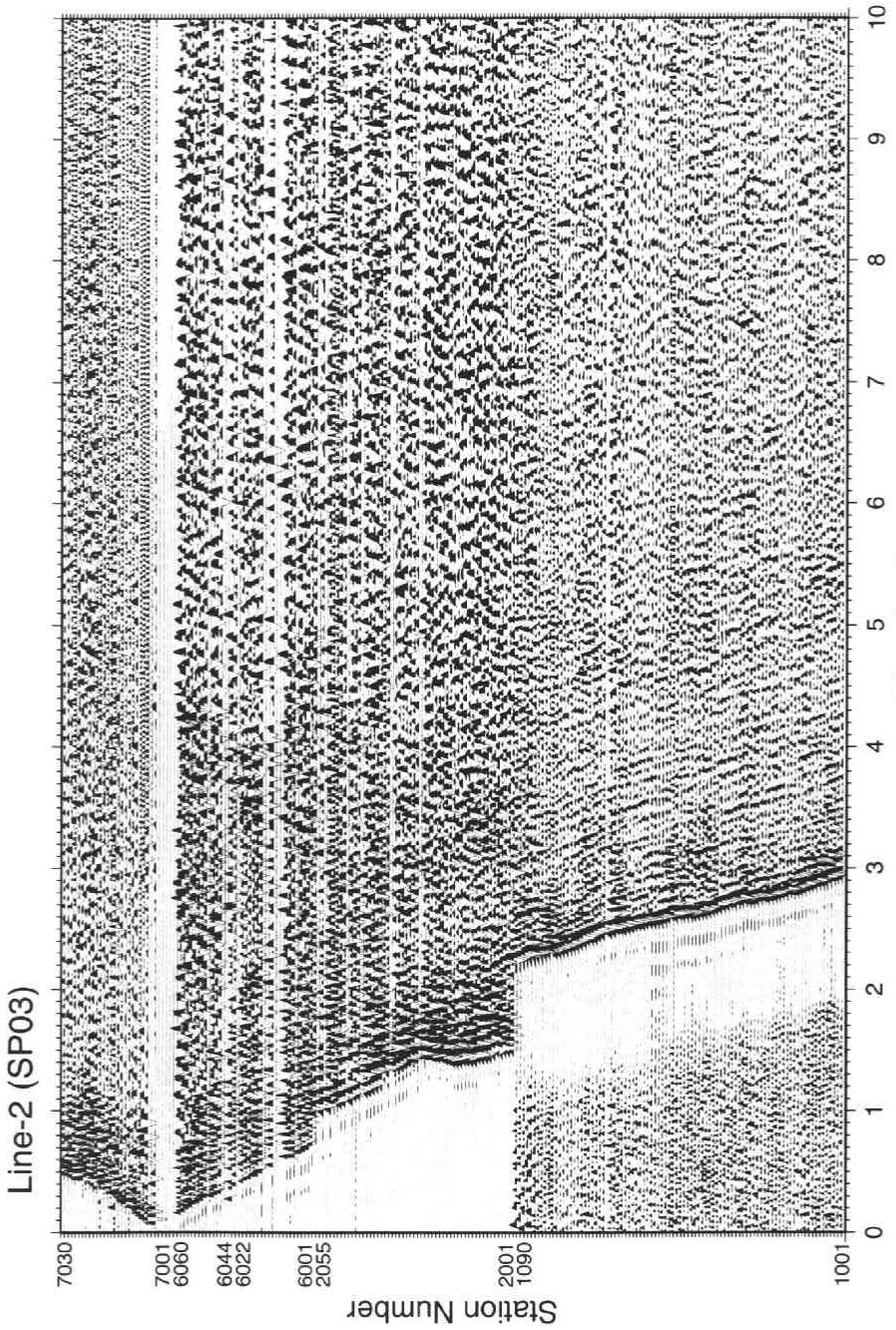

Fig. 5(c). Shot gather record sections along Line 2. Vertical component record sections from SP3.

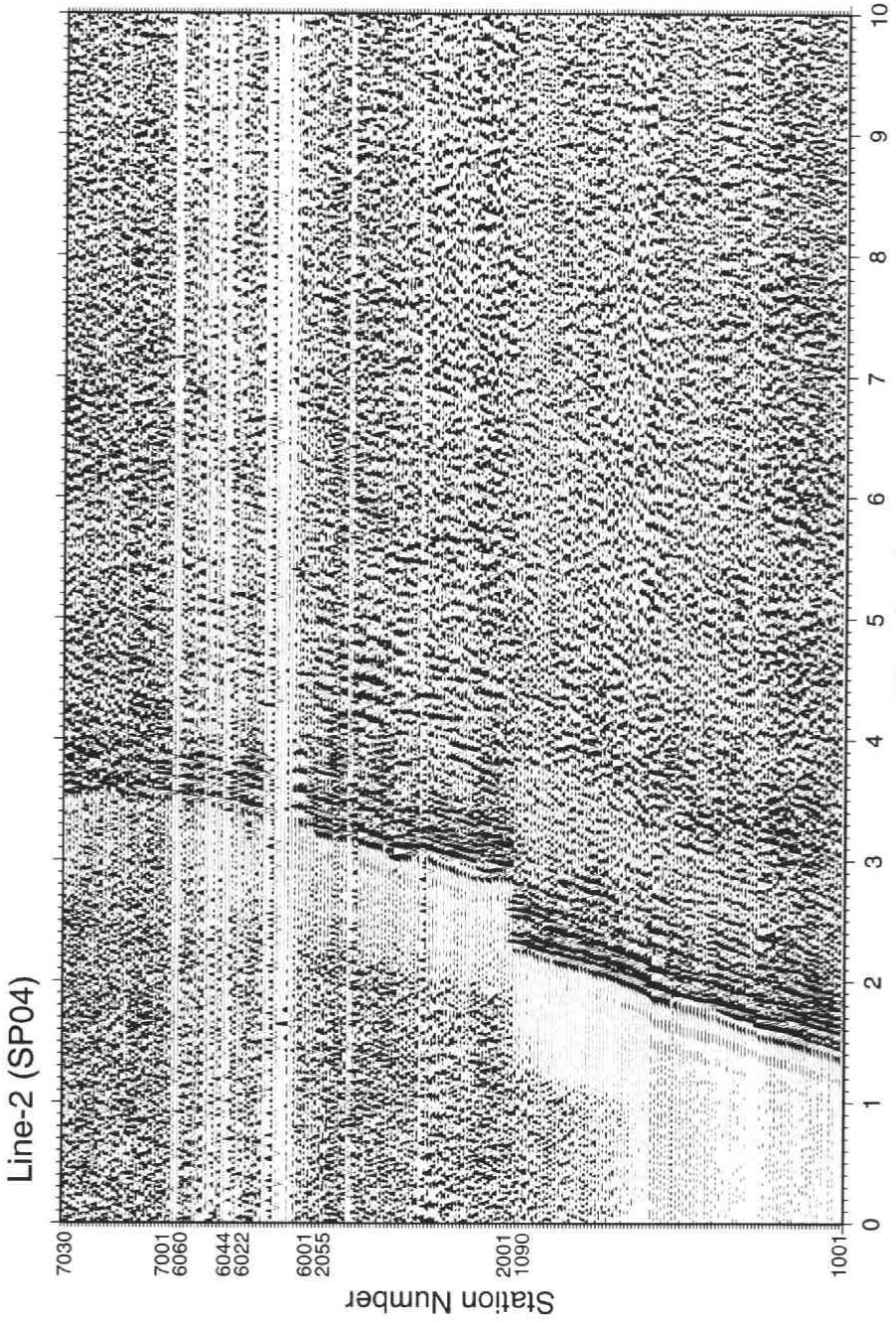

Fig. 5(d). Shot gather record sections along Line 2. Vertical component record sections from SP4.

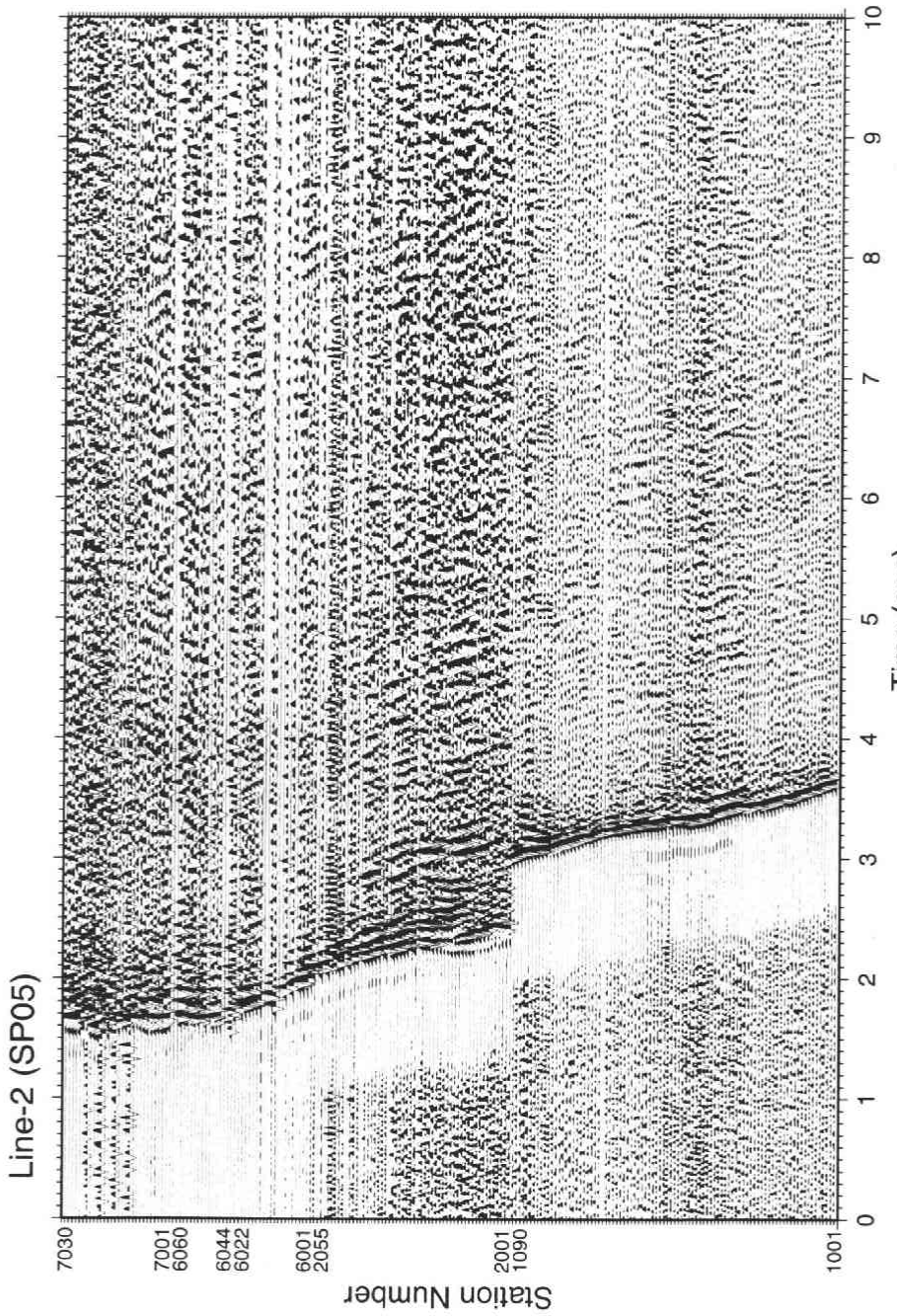

Fig. 5(e). Shot gather record sections along Line 2. Vertical-component record sections from SP5.

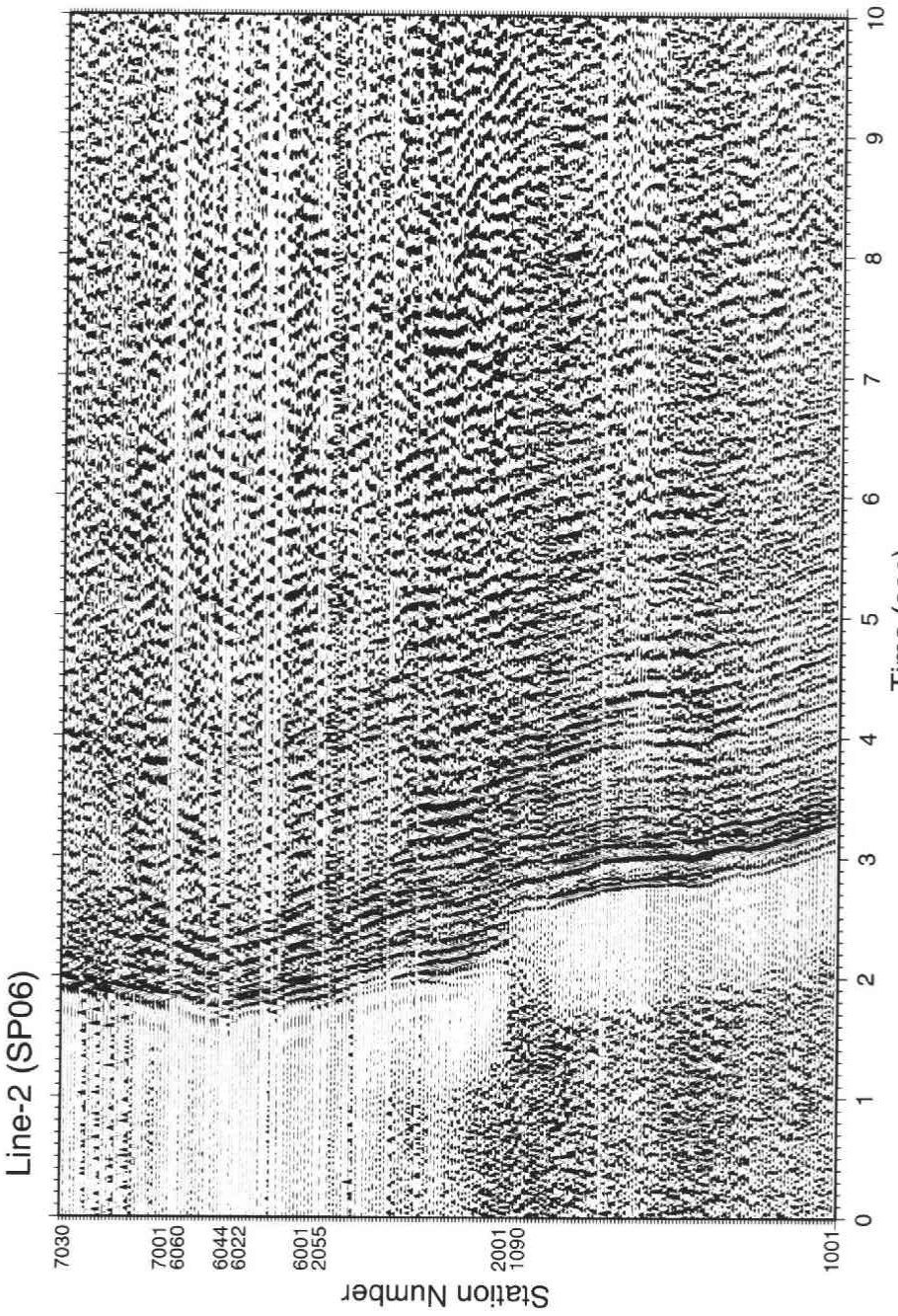

Fig. 5(f). Shot gather record sections along Line 2. Vertical-component record sections from SP6.

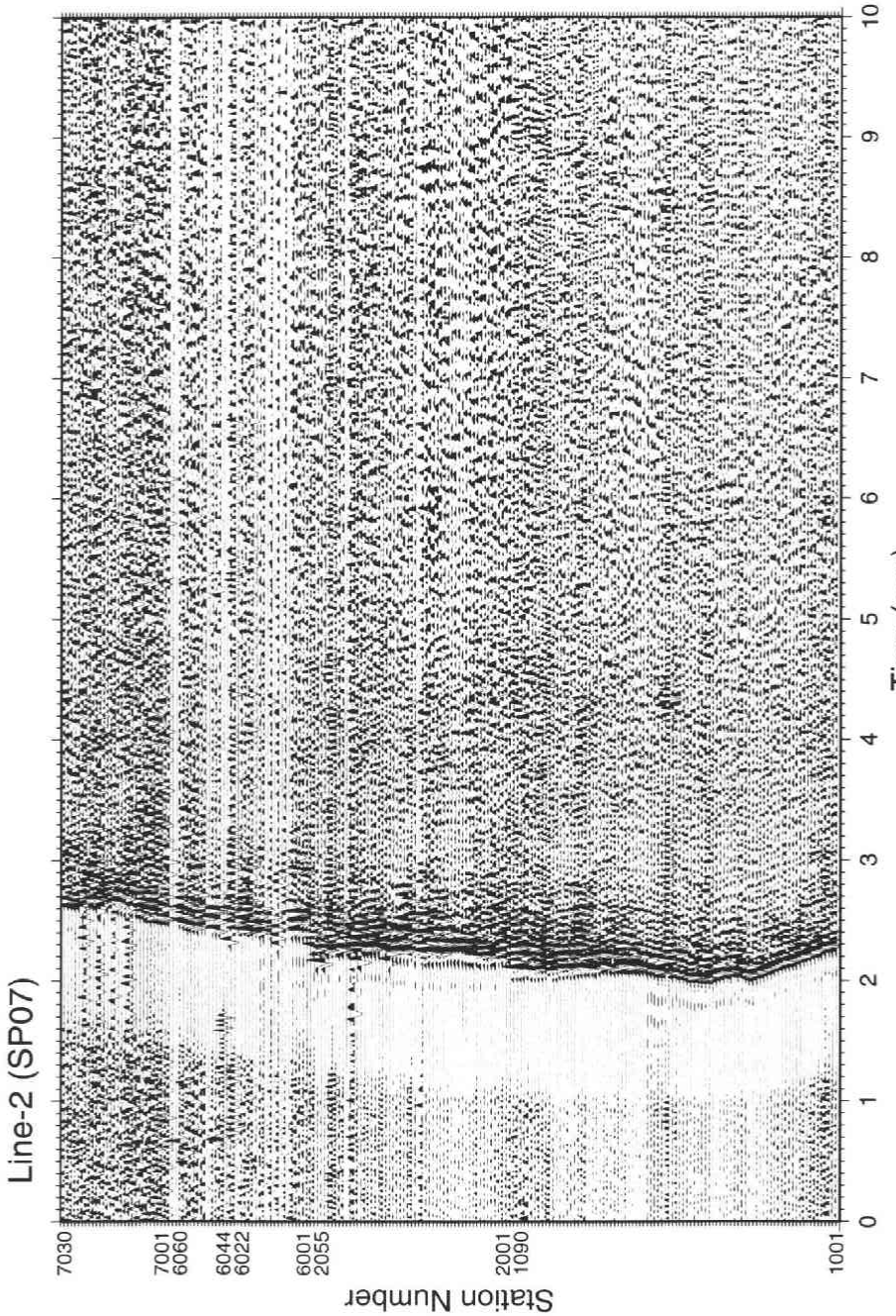

Fig. 5(g). Shot gather record sections along Line 2. Vertical-component record sections from SP7.

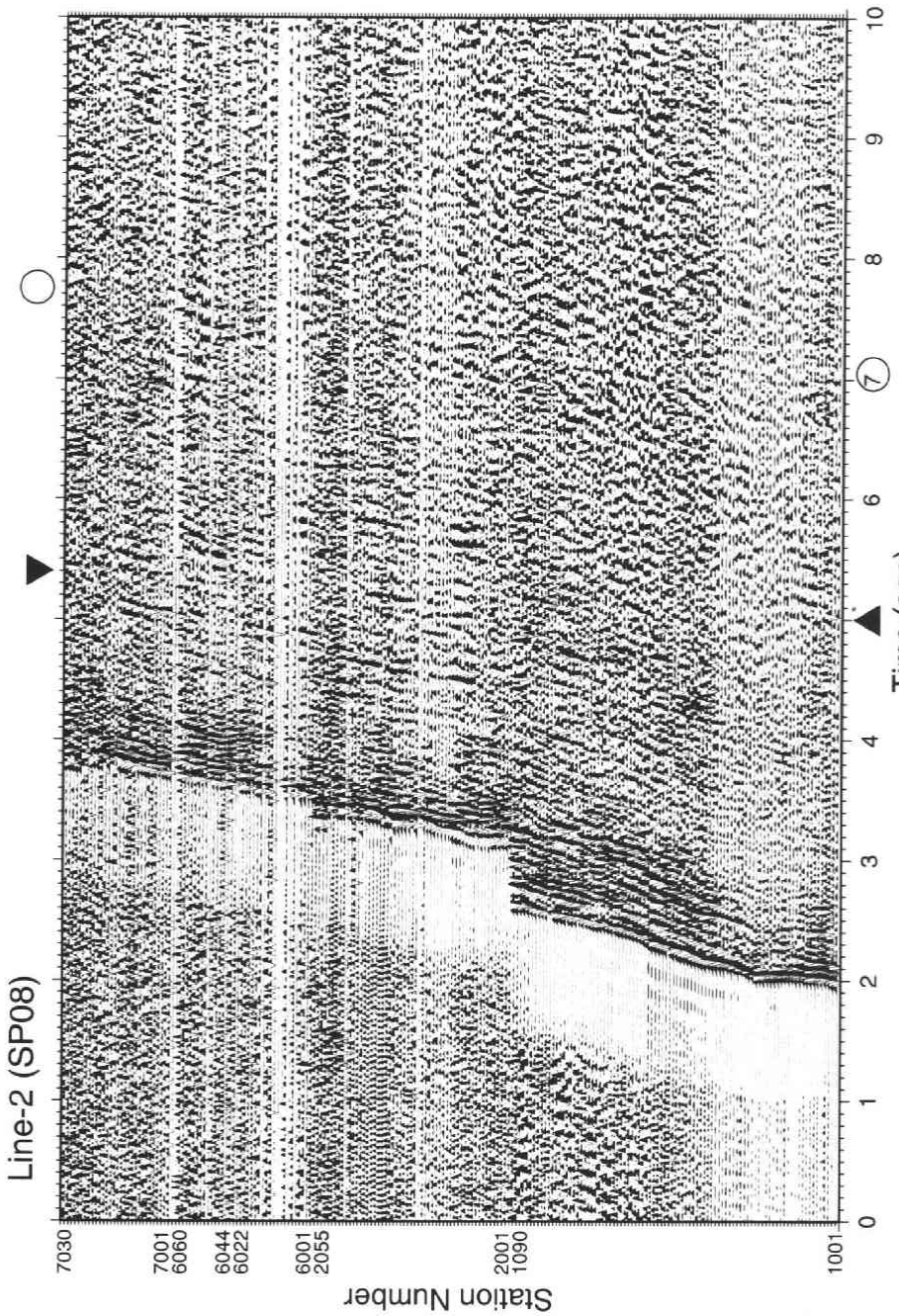

Fig. 5(h). Shot gather record sections along Line 2. Vertical-component record sections from SP8.

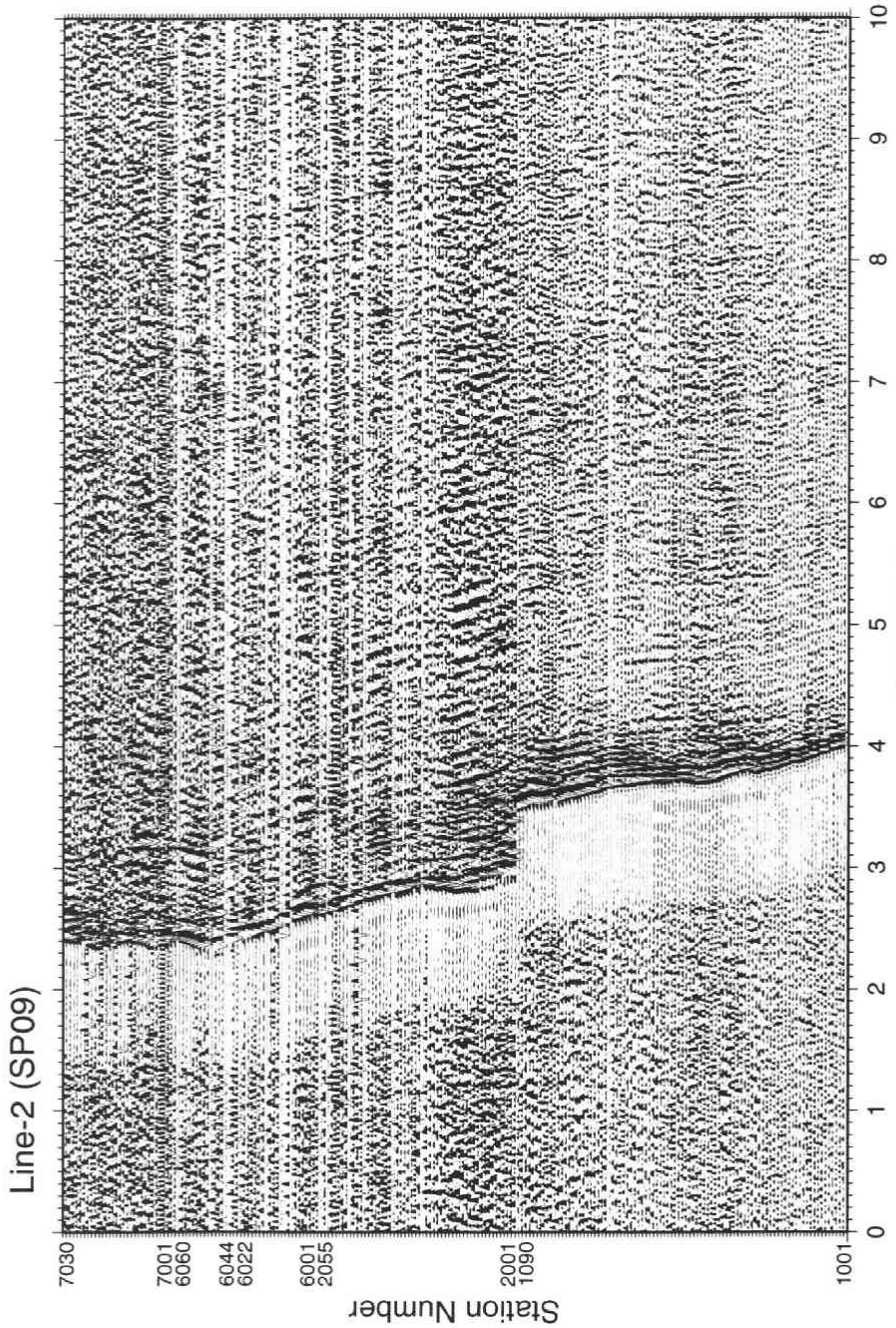

Fig. 5(i). Shot gather record sections along Line 2. Vertical-component record sections from SP9.

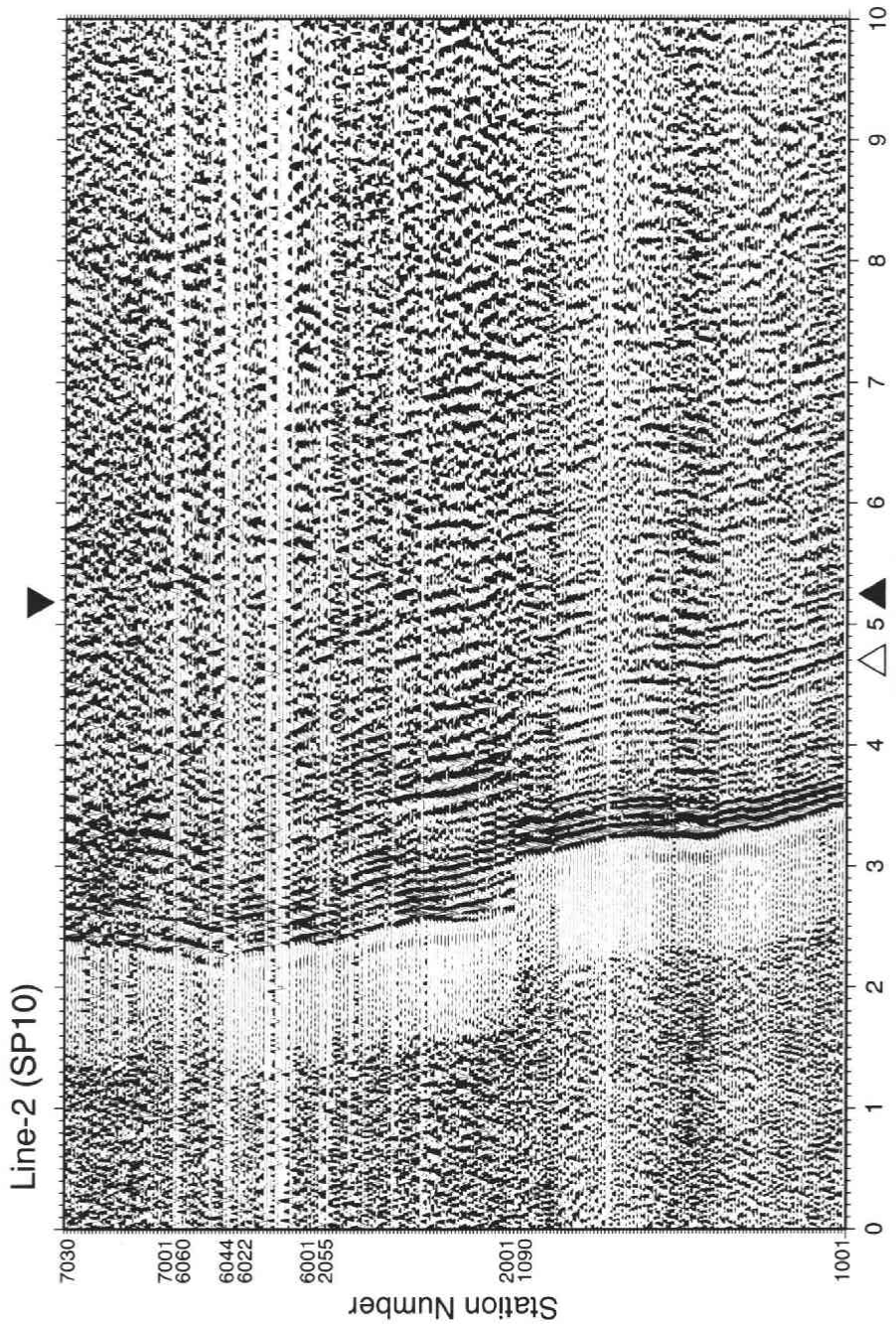

Fig. 5(j). Shot gather record sections along Line 2. Vertical-component record sections from SP10.

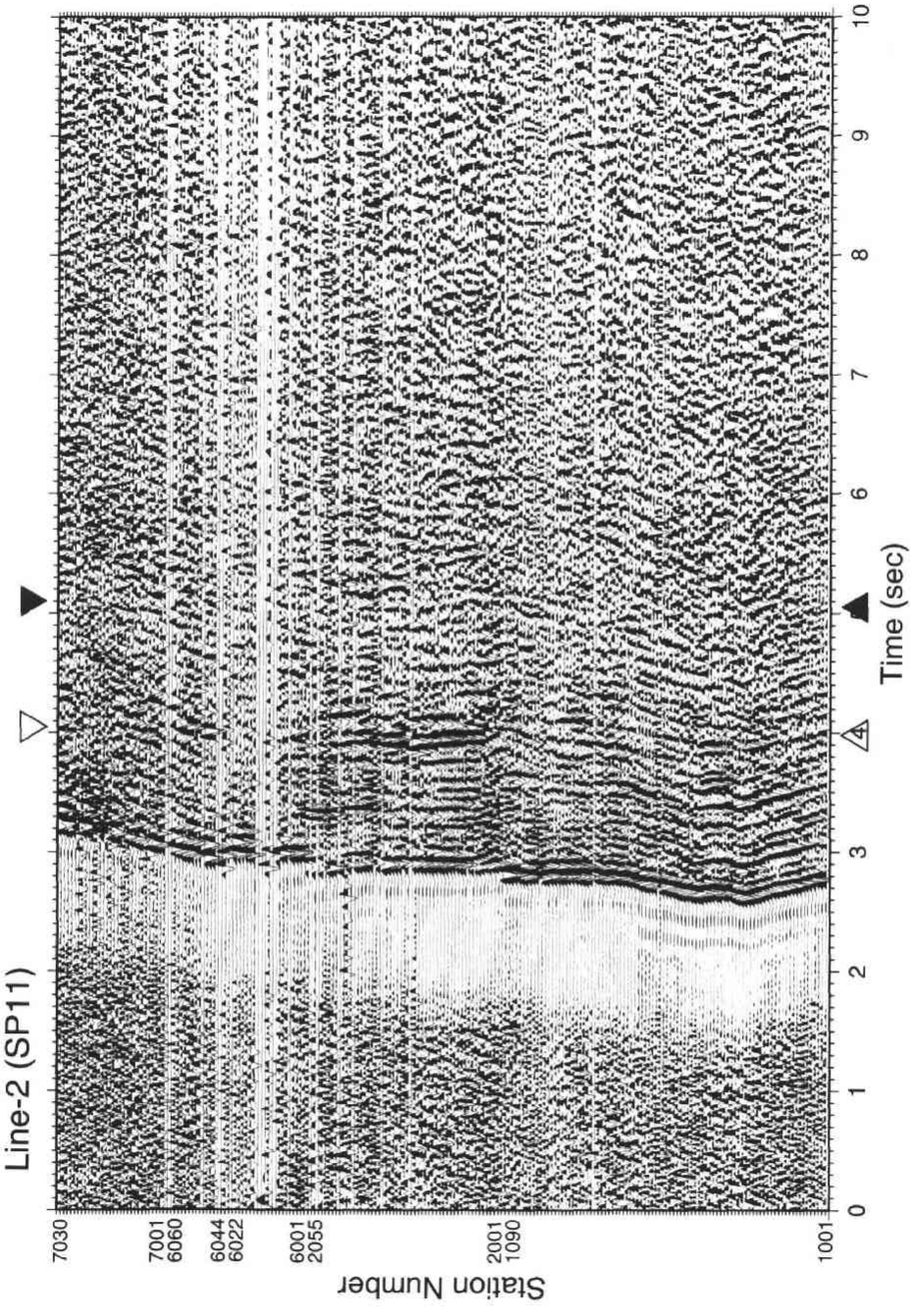

Fig. 5(k). Shot gather record sections along Line 2. Vertical-component record sections from SP11.

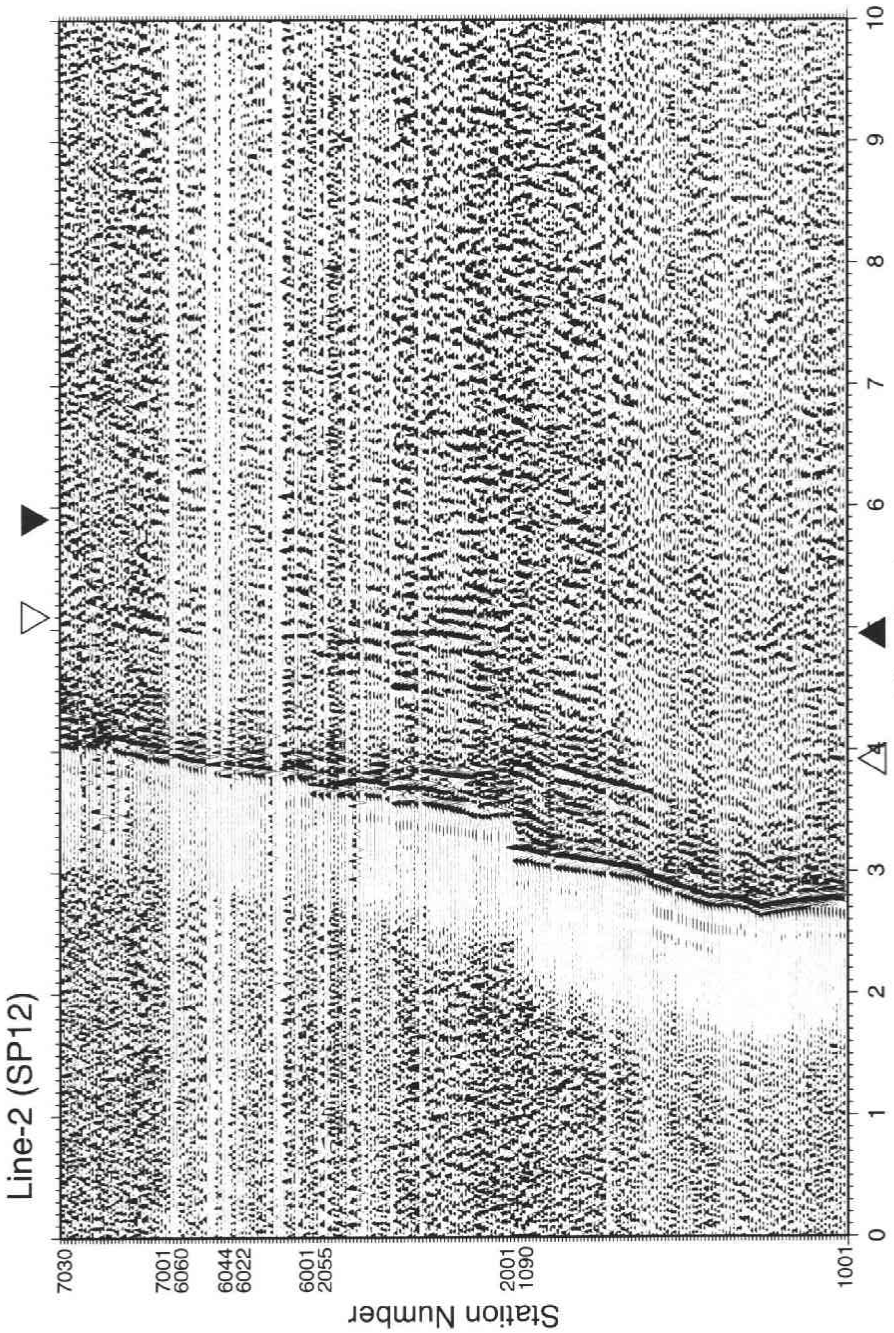

Fig. 5(l). Shot gather record sections along Line 2. Vertical-component record sections from SP12.

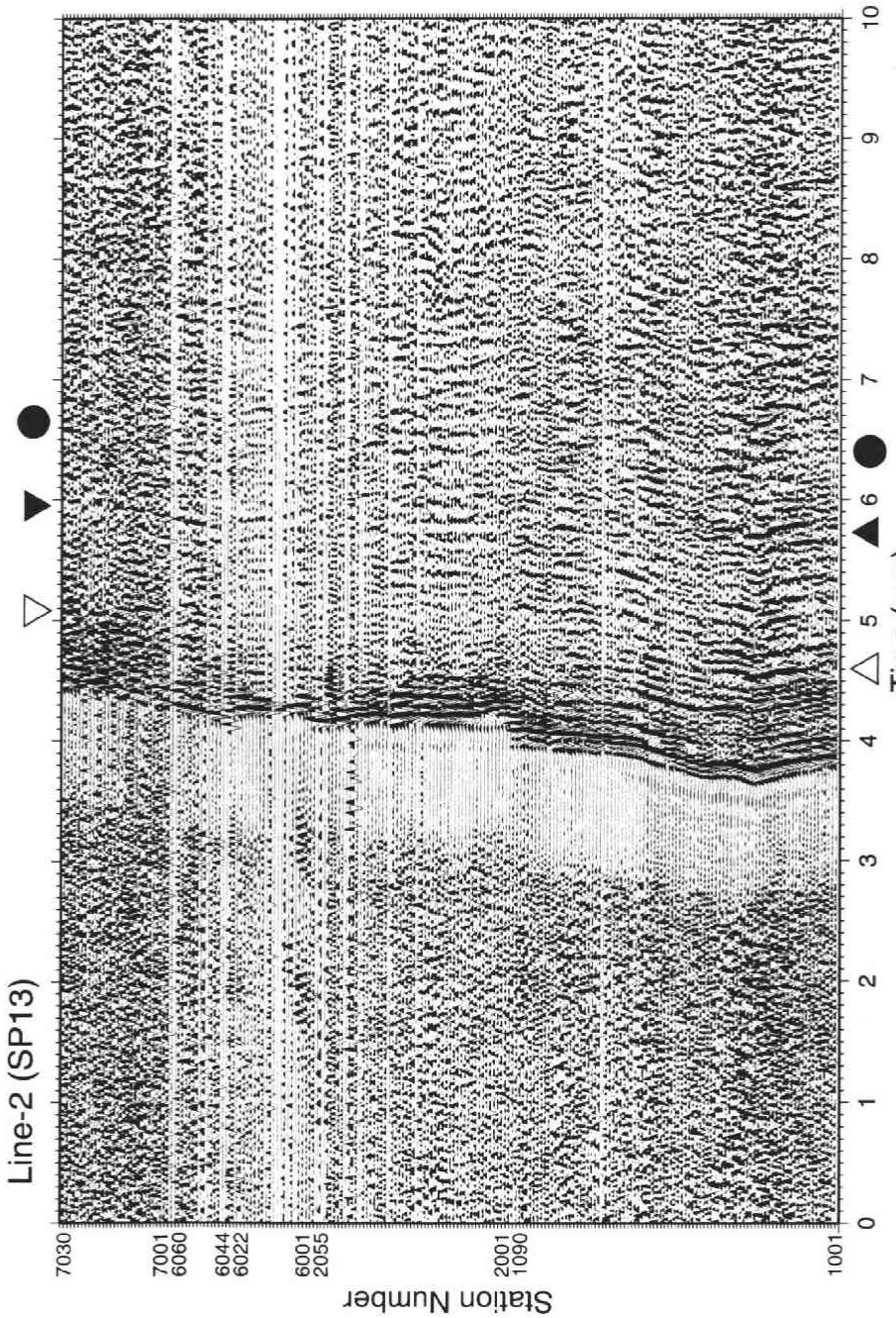

Fig. 5(m). Shot gather record sections along Line 2. Vertical-component record sections from SP13.

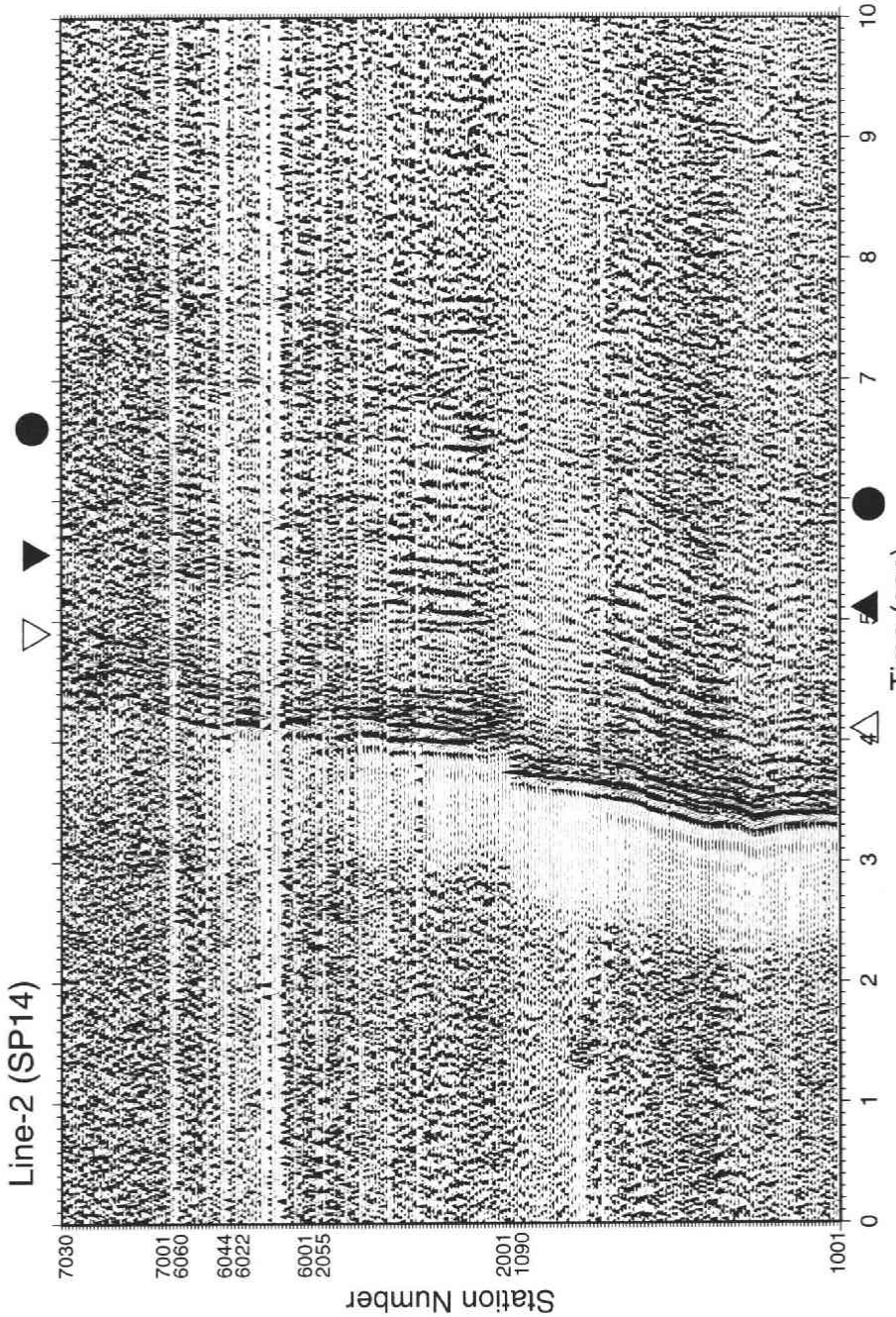

Fig. 5(n). Shot gather record sections along Line 2. Vertical-component record sections from SP14.

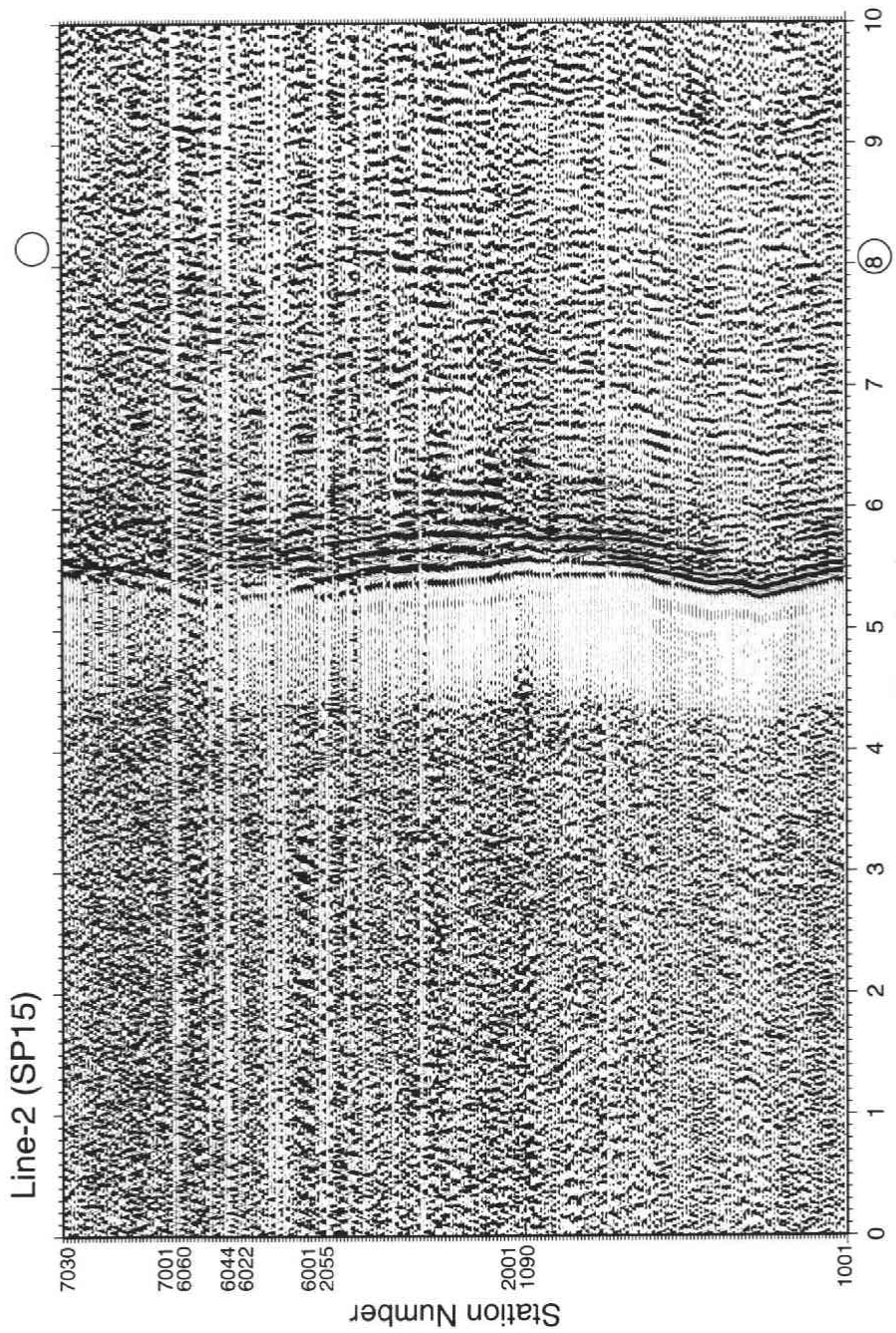

Fig. 5(o). Shot gather record sections along Line 2. Vertical-component record sections from SP15.

expected to be somewhat complicated. However, several distinct reflection events were clearly observed in the shot gather seismic record sections, and were interpreted as reflected waves from the deep structure of the Nagamachi-Rifu fault. The present seismic expedition with 368 off-line recorders is one of the largest seismic experiments ever carried out in Japan. Collaboration with the two reflection profiling receiver arrays (Line A and Line B) and other small seismic arrays will provide more important information on the deep structure in the study area.

Acknowledgments: This research was conducted as a part of comprehensive joint research project "Modeling of Deep Slip Processes in Seismogenic Inland Faults" supported by Special Coordination Funds for Promoting Science and Technology. We thank the organizations and individuals of Miyagi Prefecture and Sendai City for their cooperation in this project, and all the members who participated in the field works and data processing. We are very grateful to the staff of Japex Geoscience Institute, Inc. for giving data of surface P-wave velocities. The comments by an anonymous reviewer greatly improved the manuscript.

References

Active Fault Research Group, 1991: *Active Faults in Japan: sheet maps and inventories* (*Revised edition*) (in Japanese), 437 pp, University of Tokyo Press, Tokyo.

Ansel, J.H. and E.G.C. Smith, 1975: Detailed structure of a mantle seismic zone using homogeneous station method, *Nature*, **253**, 518-520.

Asano, Y., N. Umino, A. Nakamura, T. Okada, S. Hori, T. Kono, K. Nida, T. Sato, A. Hasegawa, M. Kosuga and A. Hasemi, 1999: Spatial distribution of seismic scatterers beneath the Ou Backbone range, northeastern Japan, estimated by seismic array observation (in Japanese), *J. Seismol. Soc. Jpn.*, **52**, 379-394.

Hasegawa, A., D. Zhao, S. Hori, A. Yamamoto and S. Horiuchi, 1991: Deep structure of the northeastern Japan arc and its relationship to seismic and volcanic activity, *Nature*, **352**, 683-689.

Hasegawa, A., A. Yamamoto, N. Umino, S. Miura, S. Horiuchi, D. Zhao and H. Sato, 2000: Seismic activity and deformation process of the crust within the overriding plate in the northeastern Japan subduction zone, *Tectonophysics*, **319**, 225-239.

Hasegawa, A., H. Ito, T. Iwasaki and T. Ikawa, 2001a: Deep structure of Nagamachi-Rifu fault as inferred from seismic expeditions, *Proceedings of International Symposium on Slip and Flow in and below the Seismogenic Region, Sendai, Nov. 5-7, 2001*, 9.

Hasegawa, A., N. Umino and S. Hori, 2001b: Seismic activity and inhomogeneous structure of the crust around the Nagamachi-Rifu fault (in Japanese), *Gekkan Chikyu*, **23**, 313-320.

Hori, S., N. Umino, Y. Asano and A. Hasegawa, 1999: S-wave reflectors in the crust of northeastern Japan (in Japanese), *Programme and Abstracts of the Seismological Society of Japan, 2001 Fall Meeting*, P140.

Ikawa, T., T. Kawanaka, S. Kawasaki, A. Hasegawa, N. Umino, A. Nakamura and H. Ito, 2001: Seismic reflection survey of the deep structure of Nagamachi-Rifu fault, Northeastern Japan, *Proceedings of International Symposium on Slip and Flow in and below the Seismogenic Region, Sendai, Nov. 5-7, 2001*, 44.

Nakamura, A. and Research Group for Deep Structure of Nagamachi-Rifu Fault, 2001: Estimation of deep fault geometry of Nagamachi-Rifu fault from seismic array observations, *Proceedings of International Symposium on Slip and Flow in and below the Seismogenic Region, Sendai, Nov. 5-7, 2001*, 45.

Okada, T. and Seismic Array Observation Group by using DAT Recorders, 1998: Seismic array observation by using DAT recorders (in Japanese), *Programme and Abstracts of the*

Seismological Society of Japan, 1998 Fall Meeting, P167.

Otsuki, K., 1999: Fundamental characteristics of Nagamachi-Rifu fault zone (in Japanese), *Programme and Abstracts of the Seismological Society of Japan, 1999 Fall Meeting*, A89.

Research Group for Deep Structure of Nagamachi-Rifu Fault, 2001: Estimation of deep structure of Nagamachi-Rifu fault—Reflection from detachment fault?—(in Japanese), *Programme and Abstracts of the Seismological Society of Japan, 2001 Fall Meeting*, C32.

Research Group for Explosion Seismology, 1999a: Seismic refraction/wide-angle experiment across the northern Honshu arc (in Japanese), *Bull. Earthq. Res. Inst.*, **74**, 63-122.

Research Group for Explosion Seismology, 1999b: Explosion seismic observations in eastern Kyushu, Japan, I, Shonai-Kushima profile (in Japanese), *Bull. Earthq. Res. Inst.*, **74**, 123-140.

Research Group for Explosion Seismology, 1999c: Explosion seismic observations in eastern Kyushu, Japan, II, Ajimu-Tano profile (in Japanese), *Bull. Earthq. Res. Inst.*, **74**, 141-160.

Umino, N., T. Okada, T. Matsuzawa, S. Hori, T. Kono, K. Nida, A. Hasegawa and N. Nishide, 1999: On M5.0 earthquake that occurred at the deepest portion of Nagamachi-Rifu Fault on September 15, 1998 (in Japanese). *Gekkan Chikyu Gougai* **27**, 148-154.

Umino, N., H. Ujikawa, S. Hori and A. Hasegawa, 2001: Distinct S-wave reflectors (bright spots) detected beneath Nagamachi-Rifu fault, *Proceedings of International Symposium on Slip and Flow in and below the Seismogenic Region, Sendai, Nov. 5-7, 2001*, 47.

Yoshida, T., 2001: The evolution of arc magmatism in the NE Honshu arc, Japan, *Tohoku Geophys. J.*, **36**, 131-149.

Yoshimoto, K., N. Uchida, H. Sato, M. Ohtake, N. Hirata and K. Obara, 2000: Microseismicity around the Nagamachi-Rifu fault, Miyagi Prefecture, northeastern Japan (in Japanese), *J. Seismol. Soc. Jpn.*, **52**, 407-416.